Correction for X- and γ-ray coincidence effects in the efficiency calibration of an n-type germanium detector

Xilei, Lin; Heydorn, Kaj

Publication date:
1991

Document Version
Publisher's PDF, also known as Version of record

RISØ

Risø-R-593

Correction for X- and γ – Ray Coincidence Effects in the Efficiency Calibration of an n-Type Germanium Detector

Lin Xilei and K. Heydorn

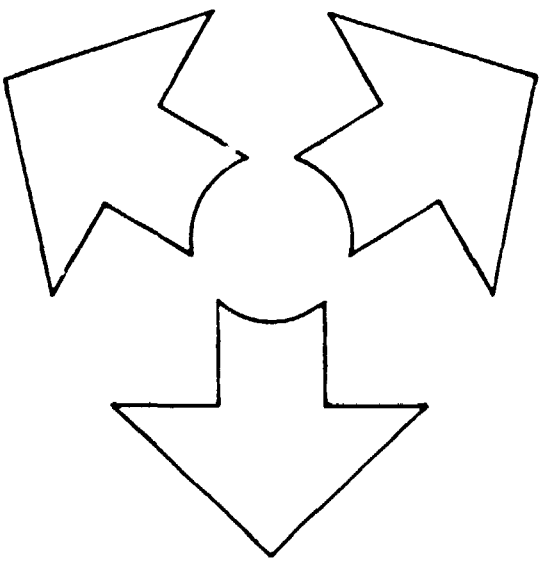

Risø National Laboratory, Roskilde, Denmark
June 1991

Correction for X- and γ – Ray Coincidence Effects in the Efficiency Calibration of an n-Type Germanium Detector

Risø-R-595

Lin Xilei* and K. Heydorn

**On leave from the General Research Institute of Non-ferrous Metals, Beijing, China*

Risø National Laboratory, Roskilde, Denmark
June 1991

Abstract

The absolute full-energy peak efficiency (ε_p) is an essential parameter in work related to the determination of gamma-ray intensities. ε_p may be determined by means of radioactive standard point sources with single or multiple gamma energies covering the range of interest. Cascade coincidence effects may be avoided by counting point sources 15 cm or more from the detector; however, the efficiency of actual samples measured at positions closer to the detector may have to be determined by means of standard sources of the same geometry and with similar main components as the actual sample.

For n-type gamma-X detectors the situation is particularly difficult. Even single gamma-ray standard sources useful for calibration of p-type gamma-ray detectors cannot always be assumed to be coincidence-free; this is due to the much higher efficiency for X-rays, resulting in gamma-X coincidence effects when counting close to an n-type detector.

This work includes the study of combinations of cascade coincidences between gamma-rays, X-rays, and 511 keV annihilation radiation, as well as β-radiation and its associated bremsstrahlung. The radionuclides ^{22}Na, ^{24}Na, ^{51}Cr, ^{54}Mn, ^{57}Co, ^{60}Co, ^{65}Zn, ^{85}Sr, ^{88}Y, ^{109}Cd, ^{113}Sn, ^{137}Cs, ^{139}Ce, ^{203}Hg, and ^{241}Am were scrutinized for potential cascade coincidences, and practical corrections were calculated.

A gamma-X detector with a relative efficiency of 35 % was calibrated with these 15 nuclides in 1 cm^3 aqueous solutions in half-dram polyethylene containers at 7 distances, ranging from 0.88 cm to 17.5 cm, with and without a perspex β-absorber between the detector and sample. After correcting for coincidences, smooth ε_p-curves were obtained for the energy range 12 to 2750 keV, even for the position closest to the detector.

ISBN 87-550-1753-3
ISSN 0106-2840

Grafisk Service - Risø - 1991

Contents

Introduction 5

Cascade Coincidence of Gamma and K X-rays 6

1. γ–γ Cascade 7

   (1) γ_1
   (2) γ_2
   (3) γ_3
   (4) Coincidence correction factor COI

2. Orbital electron capture followed by γ-transition/internal conversion 9

   (1) γ
   (2) K X-rays (K_α and K_β)

3. γ-transition preceded by β^+-decay 11

   (1) γ
   (2) KX(IC)
   (3) 511 keV

4. γ-transition preceded by β^--decay 12

   (1) γ
   (2) KX(IC)

Nuclides Used in ε_p-calibration of Gamma-X Detector 12

^{88}Y 13

   (1) 898.0 keV
   (2) 1836.1 keV
   (3) K X-rays (K_α and K_β)

^{241}Am 16

   (1) 59.5 keV
   (2) 26.3 keV
   (3) L X-rays

Experimental 21

P/T-determination 22

ε_p-determination 23

Results and Discussion 24

P/T-Curves 24

COI factors 25

ε_p-curves 28

Conclusion 29

References 31

Tables 33

Figures 37

Introduction

The absolute full-energy peak efficiency (ε_p) is an essential parameter in work related to the determination of gamma-ray intensities. This is also the case in neutron activation analyses that rely on the absolute or k_o-standardization methods. ε_p may be determined by means of radioactive standard point sources with single or multiple gamma energies covering the range of interest. Cascade coincidence effects may be avoided by counting at a distance greater than 15 cm from the detector. Under certain conditions the efficiency of actual samples measured at positions closer to the detector may be evaluated by a semiempirical method [1]. Often there is no way to calculate the efficiency accurately, and the ε_p has to be determined by using standard sources with the same geometry and main components as the actual sample.

For p-type gamma-ray detectors with an aluminium end-cap and a dead-layer of germanium crystal facing the radioactive sources, single gamma-line sources are useful for calibration even close to the detector. Many such sources contain electron-capture nuclides, which decay to an excited level and emit a cascade of low-energy K X-rays along with the gamma-ray; in practice they are considered coincidence-free, because the efficiency of such detectors at less than 50 keV drops sharply with decreasing photon energy.

For n-type gamma-X detectors the situation is different. Even single gamma-ray standard sources cannot always be assum-

ed to be coincidence-free; this is due to the much higher efficiency for X-rays, resulting in gamma-X coincidence effects when counting close to the detector.

This study includes combinations of cascade coincidences between gamma-rays, X-rays, 511 keV annihilation radiation, as well as β^--radiation and its associated bremsstrahlung. The following radionuclides ^{22}Na, ^{24}Na, ^{51}Cr, ^{54}Mn, ^{57}Co, ^{60}Co, ^{65}Zn, ^{85}Sr, ^{88}Y, ^{109}Cd, ^{113}Sn, ^{137}Cs, ^{139}Ce, ^{203}Hg, and ^{241}Am, which are frequently used in ε_p-calibration, were scrutinized for potential cascade coincidences, and practical corrections were calculated. A gamma-X detector with a relative efficiency of 35 % was calibrated with these 15 nuclides at 7 separate positions.

Cascade Coincidence of Gamma- and K X-rays

Figure 1 shows four basic cascade decay schemes often encountered in Gamma-X detector calibration work: (a) γ-γ cascade with the internal conversion (IC) K X-rays; (b) electron capture (EC) with the resulting K X-rays, KX(EC), followed by a γ-transition/internal conversion; (c) β^+ decay and its associated 511 keV annihilation radiation followed by a γ-transition/internal conversion; and (d) γ-transition/internal conversion preceded by a β^--decay and its associated bremsstrahlung. L X-rays created by electron capture/internal conversion are not considered here due to their low photon energy/intensity for the nuclides considered, apart from ^{241}Am. The L X-rays of ^{241}Am, which play an important role in the efficiency calibration at the low photon energy range, will be discussed separately in the next section.

The γ-γ coincidence effects (Fig. 1 (a)) have been investigated extensively. The line of reasoning used in this work to calculate the γ-γ coincidence correction factor, COI, was originally introduced by Moens [2]. His method was simplified and modified for arbitrary γ-γ decay schemes by Lin [3], and

extended to include the K X-rays by De Corte [4]. The present work generalizes this reasoning to include all four decay schemes shown in Fig. 1, and formulae are derived to correct for coincidence effects of any combination of gamma or x-rays. Angular correlation is not taken into account.

1. γ-γ *Cascade, Fig. 1 (a)*

(1) γ_1

Counts in the γ_1 full-energy peak can be lost by the coincidence of γ_1 with γ_2, denoted as $[\underline{\gamma_1}-\gamma_2]$, or with its internal conversion K X-rays, $[\underline{\gamma_1}-KX(IC)_{\gamma_2}]$. The coincidence probability of a detected γ_1, denoted as $P(\gamma_1)$, is the sum of the probabilities of $[\underline{\gamma_1}-\gamma_2]$ and $[\underline{\gamma_1}-KX(IC)_{\gamma_2}]$, namely

$$P(\gamma_1) = p[\underline{\gamma_1}-\gamma_2] + p[\underline{\gamma_1}-KX(IC)_{\gamma_2}] \qquad (1)$$

The individual terms can be derived as follows:

$p[\underline{\gamma_1}-\gamma_2]$ = probability that γ_1, is followed by a γ_2 transition (a_2); γ_2-ray is emitted (c_2) and detected (ε_{T,γ_2})

$$= a_2 \cdot c_2 \cdot \varepsilon_{T,\gamma 2} \qquad (2)$$

where a - branching ratio

$c = \frac{1}{1+\alpha_T}$ α_T - total internal conversion coefficient

ε_T - absolute total efficiency

and

$p[\underline{\gamma_1}-KX(IC)_{\gamma_2}]$ = probability that γ_1 is followed by a γ_2 transition (a_2); K-shell vacancy is created ($c_2 \cdot \alpha_{K2}$); K X-ray is emitted (ω_K) and (K_α or K_β) is detected ($k_\alpha \cdot \varepsilon_{T,K\alpha} + k_\beta \cdot \varepsilon_{T,K\beta}$)

$$= a_2 \cdot c_2 \cdot \alpha_{K2} \cdot \omega_K \cdot (k_\alpha \cdot \varepsilon_{T,K\alpha} + k_\beta \cdot \varepsilon_{T,K\beta}) \qquad (3)$$

where α_K - K-shell internal conversion coefficient

ω_K - K X-ray fluorescence yield

k - fraction factor of K X-ray

k_α refers to $K_{\alpha 1}$ and $K_{\alpha 2}$, k_β to $K_{\beta 1}$, and $K_{\beta 2}$

From the formulae (2) and (3)

$$P(\gamma_1) = a_2 \cdot c_2 \cdot (\varepsilon_{T,\gamma 2} + \alpha_{K2} \cdot \omega_K \cdot \sum_i k_i \cdot \varepsilon_{T,K_i}) \quad (4)$$

with $$\sum_i k_i \cdot \varepsilon_{T,K_i} = k_\alpha \cdot \varepsilon_{T,K\alpha} + k_\beta \cdot \varepsilon_{T,K\beta} \quad (5)$$

(2) γ_2

As shown in Fig. 1 (a), γ_2 is in cascade with γ_1 and its internal conversion K X-rays. The coincidence probability of a detected γ_2, $P(\gamma_2) = p[\gamma_1 - \underline{\gamma_2}] + p[KX(IC)_{\gamma_1} - \underline{\gamma_2}]$, can be derived as follows:

$p[\gamma_1 - \underline{\gamma_2}]$ = probability that γ_2 is preceded by γ_1 emission $(e_{\gamma 1}/e_{\gamma 2})$; γ_1 is detected $(\varepsilon_{T,\gamma 1})$; γ_1 is followed by γ_2 transition (a_2) and γ_2-ray is emitted (c_2)

$$= (e_{\gamma 1}/e_{\gamma 2}) \cdot a_2 \cdot c_2 \cdot \varepsilon_{T,\gamma 1} \quad (6)$$

where e - absolute emission intensity

and

$p[KX(IC)_{\gamma_1} - \underline{\gamma_2}]$ = probability that γ_2 is preceded by K X-ray emission from the γ_1 internal conversion $(e_{KX(IC)_{\gamma_1}}/e_{\gamma_2})$; the K X-rays are detected $(\sum_i k_i \cdot \varepsilon_{T,Ki})$; followed by γ_2 transition (a_2) and the γ_2-ray is emitted (c_2)

$$= (e_{KX(IC)_{\gamma 1}}/e_{\gamma 2}) \cdot a_2 \cdot c_2 \cdot \sum_i k_i \cdot \varepsilon_{T,Ki}$$

$$= (e_{\gamma 1}/e_{\gamma 2}) \cdot a_2 \cdot c_2 \cdot \alpha_{K1} \cdot \omega_K \cdot \sum_i k_i \cdot \varepsilon_{T,Ki} \quad (7)$$

with $$e_{KX(IC)_{\gamma 1}} = e_{\gamma 1} \cdot \alpha_{K1} \cdot \omega_K \quad (8)$$

So

$$P(\gamma_2) = (e_{\gamma 1}/e_{\gamma 2}) \cdot a_2 \cdot c_2 \cdot (\varepsilon_{T,\gamma 1} + \alpha_{K1} \cdot \omega_K \cdot \sum_i a_{i1} \cdot \varepsilon_{T,Ki}) \quad (9)$$

(3) γ_3

As shown in Fig. 1 (a), the counts in γ_3 full-energy peak will be increased by coincidence of γ_1-γ_2, if both γ_1 and γ_2 are totally absorbed by the detector. The summing probability, $P^{sum}(\gamma_3)$, can be calculated as follows [3]

$$P^{sum}(\gamma_3) = \frac{e_{\gamma 1}}{e_{\gamma 3}} \cdot a_2 \cdot c_2 \cdot \frac{\varepsilon_{p,\gamma 1} \cdot \varepsilon_{p,\gamma 2}}{\varepsilon_{p,\gamma 3}} \quad (10)$$

(4) Coincidence correction factor COI

The coincidence correction factor, COI, is defined as

$$COI = \frac{N_p(exp)}{N_p} \quad (11)$$

where $N_p(exp)$ and N_p are counts of a full-energy peak experimentally observed and corrected for coincidence effects, respectively;

the COI is now calculated as [2]

$$COI = (1 - P) \cdot (1 + P^{sum}) \quad (12)$$

2. Orbital electron capture followed by γ-transition/internal conversion Fig. 1 (b)

Figure 1 (b) shows that the γ-line and its internal conversion K X-rays are in cascade with the K X-rays created by electron capture, KX(EC).

(1) γ

Following a reasoning similar to that above for the γ–γ coincidence calculation, the coincidence probability of the γ-line with the KX(EC), $P(\gamma) = p[KX(EC) - \underline{\gamma}]$, can be derived as

$$P(\gamma) = p[KX(EC) - \underline{\gamma}]$$
$$= (e_{KX(EC)}/e_\gamma) \cdot a \cdot c \cdot \sum_i \varepsilon_{\gamma,Ki}$$
$$= \frac{\varepsilon(EC) \cdot P_K \cdot \omega_K}{e_\gamma} \cdot a \cdot c \cdot \sum_i \varepsilon_{\gamma,Ki} \qquad (13)$$

$$\text{with } e_{KX(EC)} = \varepsilon(EC) \cdot P_K \cdot \omega_K \qquad (14)$$

where $\varepsilon(EC)$ – branch ratio of orbital electron capture

P_K – relative probability of electron capture in K-shell

Note that $e_{KX(EC)}$ is the K X-ray intensity from a specified EC decay branch; it differs from the K X-ray emission intensity e_{KX}, given in the literature for any nuclide, which is the total K X-ray intensity created by all EC branches and internal conversions.

(2) K X-rays (K_α and K_β)

Fig. 1 (b) shows that KX(IC), K X-rays from the internal conversion, are in cascade with KX(EC), the K X-ray from the electron capture, and KX(EC) is in cascade separately with γ and KX(IC). The coincidence probabilities of KX(IC) and KX(EC), p(KX(IC)) and p(KX(EC)) can be calculated separately as follows:

$$p(KX(IC)) = p[KX(EC) - \underline{KX(IC)}]$$
$$= (e_{KX(EC)}/e_{KX(IC)}) \cdot a \cdot c \cdot \alpha_K \cdot \omega_K \cdot \sum_i \varepsilon_{\gamma,Ki}$$
$$= \frac{\varepsilon(EC) \cdot P_K}{e_\gamma} \cdot a \cdot c \cdot \omega_K \cdot \sum_i \varepsilon_{\gamma,Ki} \qquad (15)$$

and

$$p(KX(EC)) = p[\underline{KX(EC)} - \gamma] + P[\underline{KX(EC)} - KX(IC)]$$
$$= a \cdot c \cdot (\varepsilon_{\tau,\gamma} + \alpha_K \cdot \omega_K \cdot \sum_i \varepsilon_{\tau,Ki}) \quad (16)$$

The averaged coincidence probability, P(KX), for a detected K X-ray, regardless of its origin, can be calculated as

$$P(KX) = p(KX(EC)) \cdot R_{KX(EC)} + p(KX(IC)) \cdot R_{KX(IC)} \quad (17)$$

$$\text{with } R_{KX(EC)} = \frac{e_{KX(EC)}}{e_{KX(EC)} + e_{KX(IC)}} = \frac{\varepsilon(EC) \cdot P_K}{\varepsilon(EC) \cdot P_K + e_\gamma \cdot \alpha_K} \quad (18)$$

$$R_{KX(IC)} = \frac{e_{KX(IC)}}{e_{KX(EC)} + e_{KX(IC)}} = \frac{e_\gamma \cdot \alpha_K}{\varepsilon(EC) \cdot P_K + e_\gamma \cdot \alpha_K} \quad (19)$$

3. γ-transition preceded by β⁺-decay, Fig. 1 (c)

(1) γ

The γ-ray is in coincidence with the 511-keV annihilation from the β⁺-decay. Taking into account that two 511-keV photons are emitted from one β⁺-annihilation event, the probability of a γ-ray coincidence, P(γ), is calculated as

$$P(\gamma) = p[511-\gamma]$$
$$= (e_{511}/e_\gamma) \cdot a \cdot c \cdot \varepsilon_{\tau 511}$$
$$= (2\varepsilon(\beta^+)/e_\gamma) \cdot a \cdot c \cdot \varepsilon_{\tau 511} \quad (20)$$

with $e_{511} = 2 \cdot \varepsilon(\beta^+)$

where $\varepsilon(\beta^+)$ is the β⁺-decay branching ratio

Note that the e_{511} here is the 511-keV emission intensity from the specified β⁺-decay branch, excluding that of any other possible β⁺-decay branches (to the ground level of the nuclide, for example), which also results in 511 keV annihilation radiation.

(2) KX(IC)

$$P(KX(IC)) = p[511 - \underline{KX(IC)}]$$
$$= (e_{511}/e_{KX(IC)}) \cdot a \cdot c \cdot \alpha_K \cdot \omega_K \cdot \varepsilon_{\tau 511}$$
$$= (2\varepsilon(\beta^+)/e_\gamma) \cdot a \cdot c \cdot \varepsilon_{\tau 511} \quad (21)$$

(3) 511 keV

$$P(511) = p[\underline{511} - \gamma] + p[\underline{511} - KX(IC)]$$
$$= a \cdot c \cdot (\varepsilon_{\tau,\gamma} + \alpha_K \cdot \omega_K \cdot \textstyle\sum_i \alpha_i \cdot \varepsilon_{\tau,ki}) \quad (22)$$

4. γ-transition preceded by β^--decay, Fig. 1 (d)

(1) γ

$$P(\gamma) = p[\beta^- - \underline{\gamma}]$$
$$= (e_{\beta^-}/e_\gamma) \cdot a \cdot c \cdot \varepsilon_{\tau,\beta^-}$$
$$= (\varepsilon(\beta^-)/e_\gamma) \cdot a \cdot c \cdot \varepsilon_{\tau,\beta^-} \quad (23)$$

with $e_{\beta^-} = \varepsilon(\beta^-)$

where $\varepsilon(\beta^-)$ - branching ratio of the specified β^--decay

(2) KX(IC)

$$P(KX(IC)) = p[\beta^- - \underline{KX(IC)}]$$
$$= (e_{\beta^-}/e_{KX(IC)}) \cdot a \cdot c \cdot \alpha_K \cdot \omega_K \cdot \varepsilon_{\tau,\beta^-}$$
$$= (\varepsilon(\beta^-)/e_\gamma) \cdot a \cdot c \cdot \varepsilon_{\tau,\beta^-} \quad (24)$$

Nuclides Used in ε_p-calibration of a Gamma-X Detector

In this section, 15 nuclides that were applied in the ε_p-calibration of a gamma-X detector were investigated for the potential cascade coincidences of all their important gamma- and X-rays covering the energy range of 12 to 2754 keV. Figures 2-16 provide the decay schemes and the related nuclear parameters of the 15 nuclides, simplified to suit the needs of this work.

These data were extracted from Refs. [5-8], unless otherwise indicated. For easy use of these nuclides in ε_p-related work, appropriate formulae are provided along with the figures where needed to calculate a coincidence correction factor COI. These formulae are based on the discussion in the preceding section, excluding K X-rays with energies lower than 11 keV (^{22}Na, ^{51}Cr, ^{54}Mn, ^{57}Co and ^{65}Zn), as well as β^--γ coincidences with maximum β^--energy lower than about 300 keV (^{60}Co and ^{203}Hg).

With the amplifier shaping time set at 6 μs, as used in the present work, half-lives of metastable γ-levels of 1 μs (^{85}Sr) or shorter (^{57}Co, ^{139}Ce and ^{241}Am) may be disregarded [4]. Levels with half-lives on the order of seconds or more (^{109}Cd, ^{113}Sn and ^{137}Cs), on the other hand, do not contribute to cascade coincidences.

Altogether 6 of the nuclides are thus considered coincidence-free under practical conditions of measurement, and no formulae for calculating COI are therefore included in Figs. 4, 5, 8, 11, 13, and 15, corresponding to the radionuclides ^{51}Cr, ^{54}Mn, ^{65}Zn, ^{109}Cd, ^{137}Cs, and ^{203}Hg, respectively.

The actual procedure used for generating coincidence correction formulae for individual radionuclides is illustrated in detail for ^{88}Y and ^{241}Am. The calculation of coincidence probabilities for nuclides with multiple/branch decay cascades was presented in Ref. [3].

^{88}Y

As shown in Fig. 10, γ-lines, 898.0 keV and 1836.1 keV, and K X-rays form cascades. K X-rays from the internal conversion of 898.0 keV and 1836.1 keV are negligible. The intensity of 511-keV annihilation is very weak, so its contribution to the coincidence effect of 1836.1 keV is ignored.

(1) 898.0 keV

The 898.0 keV γ-line is in cascade with KX(EC879) and the 1836.1 keV γ-line. The coincidence probability, P(898.0 keV), can be calculated as

$$P(898.0\ \text{keV}) = p[KX(EC879.0) - \underline{898.0}] + [\underline{898.0} - 1836.1] - p[KX(879) - \underline{898.0} - 1836.1]$$

$$= \frac{\varepsilon(879)\cdot P_K\cdot\omega_K}{e_{898.0}}\cdot(a\cdot c)_{898.0}\cdot\sum_i k_i\cdot\varepsilon_{T,Ki}+(a\cdot c)_{1836.1}\cdot\varepsilon_{T1836.1}$$

$$-\frac{\varepsilon(879)\cdot P_K\cdot\omega_K}{e_{898.0}}\cdot(a\cdot c)_{898.0}\cdot(a\cdot c)_{1836.1}\cdot\left(\sum_i k_i\cdot\varepsilon_{T,Ki}\right)\cdot\varepsilon_{T1836.1}$$

$$= (0.5253\ \varepsilon_{T14.4}+0.0856\ \varepsilon_{T15.88})\cdot(1-\varepsilon_{T1836.1})+\varepsilon_{T1836.1} \qquad (25)$$

(2) 1836.1 keV

As shown by the ^{88}Y decay scheme, the 1836.1 keV γ-line is in cascade with KX(EC879) and the 898.0 keV line with KX(EC1777). The total coincidence probability P(1836.1 keV), can be expressed as follows:

$$P(1836.1\ \text{keV}) = p[KX(EC879)-\underline{1836.1}]+p[898.0-\underline{1836.1}]-p[KX(EC879)-898.0-\underline{1836.1}]+p[KX(EC1777)-\underline{1836.1}]$$

$$= \frac{\varepsilon(879)\cdot P_K\cdot\omega_K}{e_{1836.1}}\cdot a_{898.0}\cdot(a\cdot c)_{1836.1}\cdot\sum_i k_i\cdot\varepsilon_{T,Ki}$$

$$+\frac{e_{898.0}}{e_{1836.1}}\cdot(a\cdot c)_{1836.1}\cdot\varepsilon_{T898.0}-\frac{\varepsilon(879)\cdot P_K\cdot\omega_K}{e_{1836.1}}\cdot(a\cdot c)_{898.0}\cdot(a\cdot c)_{1836.1}\cdot\left(\sum_i k_i\cdot\varepsilon_{T,Ki}\right)\varepsilon_{T898}$$

$$+\frac{\varepsilon(1777)\cdot P_K\cdot\omega_K}{e_{1836.1}}\cdot(a\cdot c)_{1836.1}\sum_i k_i\cdot\varepsilon_{T,Ki}$$

$$= (0.6101-0.5786\ \varepsilon_{T898.0})\cdot(0.8599\ \varepsilon_{T14.14}+0.1401\ \varepsilon_{15.88})+0.9471\varepsilon_{T898.0} \qquad (26)$$

(3) K X-rays (K_α and K_β)

As shown in Fig. 10, there are two cascade chains related respectively to KX(EC879) and KX(EC1777). The average coincidence probability of K X-rays, P(KX), is calculated as follows (refer to Eq. 17):

$$P(KX) = p(KX(EC879)) \cdot R_{KX(EC879)} + p(KX(EC1777)) \cdot R_{KX(EC1777)}$$

$$\text{with } R_{KX(EC879)} = \frac{e_{KX(EC879)}}{e_{KX(EC879)} + e_{KX(EC1777)}}$$

$$= \frac{\varepsilon(879) \cdot PK879}{\varepsilon(879) \cdot P_{K879} + \varepsilon(1777) \cdot P_{K1777}} = 0.948$$

$$R_{KX(EC1777)} = \frac{e_{KX(EC1777)}}{e_{KX(EC879)} + e_{KX(EC1777)}} = 0.0511$$

$$p(KX(EC879)) = p[\underline{KX(879)} - 898.0] + p[\underline{KX(879)} - 1836.1] - p[\underline{KX(879)} - 898.0 - 1836.1]$$

$$= (a \cdot c)_{898.0} \cdot \varepsilon_{T898.0} + a_{898.0} \cdot (a \cdot c)_{1836.1} \cdot \varepsilon_{T1836.1} - (a \cdot c)_{898.0} \cdot (a \cdot c)_{1836.1} \cdot \varepsilon_{T898.0} \cdot \varepsilon_{T1836.1}$$

$$= 0.9933\ \varepsilon_{T898.0} + 0.9936\ \varepsilon_{T1836.1} - 0.9933\ \varepsilon_{T898.0} \cdot \varepsilon_{T1836.1} \quad (27)$$

and

$$p(KX(EC1777) = (a \cdot c)_{1836.1} \cdot \varepsilon_{T1836.1} = \varepsilon_{T1836.1} \quad (28)$$

Finally

$$P(KX) = 0.9425\ \varepsilon_{T898.0} \cdot (1 - \varepsilon_{T1836.1}) + 0.9939\ \varepsilon_{T1836.1} \quad (29)$$

^{241}Am

In the simplified decay scheme of ^{241}Am presented in Fig. 16, α-decays with branching ratios (ε(α)) less than 1.5 % are omitted along with less important γ-lines with intensities (e_γ) lower than 0.05 %. In the ε_p-determination at the low energy range, the 59.5 and 26.3 keV γ-lines are often used together with the L X-rays. Figure 16 shows that these γ- and X-rays are subject to cascade coincidence effects.

L X-rays of ^{237}Np, the α-decay product of ^{241}Am, originate from the internal conversion of the corresponding γ-transitions, as shown in Fig. 16. The L X-ray intensity may be written as follows:

$$e_{LX} = e_\gamma \cdot (\alpha_L + \alpha_K \cdot n_{KL}) \cdot \bar{\omega}_L \qquad (30)$$

where α_L and α_K - L- and K-shell internal conversion coefficients, respectively

n_{KL} - the total number of L-vacancies created by K → L vacancy transfer

$\bar{\omega}_L$ - the mean L-shell fluorescence yield

Since the γ-transition energies concerned here are insufficient to produce K X-rays of ^{237}Np (the lowest K X-ray energy, $EK_{\alpha 2}$, is 97 keV), the intensity of the conversion L X-rays may be rewritten as

$$e_{LX} = e_\gamma \cdot \alpha_L \cdot \bar{\omega}_L \qquad (31)$$

In fact, the K X-rays of ^{237}Np are extremely weak. They are produced by the γ-transitions with higher energy but with very low intensities, which are omitted in Fig. 16. Compared with the L X-rays intensity e_{LX} = 39.54 %, the K X-ray intensity is only 0.0040 % [10]. Consequently, the contribution to the L X-rays from K-vacancies giving rise to K → L vacancy transfer is negligible in this context.

A calculation based on Eq. 31 shows that the four γ-transitions presented in Fig. 16 produce 28 % of the total L X-rays. In other words, the simplified decay scheme of ^{241}Am will be adequate for making the following calculations:

(1) 59.5 keV

The summing effect on 59.5 keV by full-coincidence of 26.3 keV with 33.2 keV is negligible because of the very low intensities associated with these lines. The calculation of ^{sum}P based on Eq. (10) showed that the effect is never higher than 1 %.

The coincidence loss of 59.5 keV with 43.4 keV and its internal conversion L X-rays can be calculated as follows:

$$P(59.5\ keV) = p[43.4/LX_{43.4} - \underline{59.5}]$$

$$= \frac{e_{43.4}}{e_{59.5}} \cdot (a \cdot c)_{59.5} \cdot (\varepsilon_{T43.4} + \alpha_{L43.4} \cdot \bar{\omega}_L \cdot \sum_i k_i \cdot \varepsilon_{T,Li})$$

$$= 8.5 \cdot 10^{-4}\ \varepsilon_{T43.4} + 0.0552 \sum_i k_i \cdot \varepsilon_{T,Li} \qquad (32)$$

with

$$\sum_i k_i \cdot \varepsilon_{T,Li} = 0.0205\ \varepsilon_{T11.87} + 0.3288\ \varepsilon_{T13.93} + 0.5192\ \varepsilon_{T17.58} + 0.1315\ \varepsilon_{T21.0} \qquad (33)$$

(2) 26.3 keV

26.3 keV γ-line is in cascade with 43.4 and 33.2 keV, as well as with their conversion L X-rays.

$$P(26.3\ keV) = p[43.4/LX_{43.4} - \underline{26.3}] + p[\underline{26.3} - 33.2/LX_{33.2}] - p[43.4/LX_{43.4} - \underline{26.3} - 33.2/LX_{33.2}] \qquad (34)$$

with

$$p[43.4/LX_{43.4} - \underline{26.3}] = \frac{e_{43.4}}{e_{26,3}} \cdot (a \cdot c)_{26.3} \cdot (\varepsilon_{T26.3} + \alpha_{L43.4} \cdot \bar{\omega}_L \cdot \sum_i k_i \cdot \varepsilon_{T,Li})$$

$$= 2.1 \cdot 10^{-4}\ \varepsilon_{T26.3} + 0.01383 \sum_i k_i \cdot \varepsilon_{T,Li} \qquad (35)$$

$$p[\underline{26.3}\text{-}33.2/KL_{33.2}] = (a\cdot c)_{33.2}\cdot(\varepsilon_{T33.2}+\alpha_{L33.2}\cdot\bar{\omega}_L\cdot\sum_i k_i\cdot\varepsilon_{T,Li})$$

$$= 5.38\cdot10^{-3}\ \varepsilon_{T33.2} + 0.3903\ \sum_i k_i\cdot\varepsilon_{T,Li} \qquad (36)$$

$$p[43.4/LX_{43.4} - \underline{26.3} - 33.2/LX_{33.2}]$$

$$= \frac{e_{43.4}}{e_{26.3}}\cdot(a\cdot c)_{26.3}\cdot(a\cdot c)_{33.2}\cdot(\varepsilon_{T43.4}+\alpha_{L43.4}\cdot\bar{\omega}_L\cdot\sum_i k_i\cdot\varepsilon_{T,Li})\cdot(\varepsilon_{T33.2}+\alpha_{L33.2}\cdot\bar{\omega}_L\cdot\sum_i k_i\cdot\varepsilon_{T,Li})$$

$$= 1.14\cdot10^{-6}\ \ (\varepsilon_{T43.4} + 65.22\ \sum_i k_i\cdot\varepsilon_{T,Li})\cdot(\varepsilon_{T33.2} + 72.59\ \sum_i k_i\cdot\varepsilon_{T,Li}) \qquad (37)$$

So

$$P(26.3\ \text{keV}) = 2.1\cdot10^{-4}\ \varepsilon_{T26.3} + 5.38\cdot10^{-3}\ \varepsilon_{T33.2} + 0.404\ \sum_i k_i\cdot\varepsilon_{T,Li}$$
$$- 1.14\cdot10^{-6}\ \ (\varepsilon_{T43.4} + 65.22\ \sum_i k_i\cdot\varepsilon_{T,Li})\cdot(\varepsilon_{T33.2} + 72.59\ \sum_i k_i\cdot\varepsilon_{T,Li}) \qquad (38)$$

(3) L X-rays

As discussed above, more than 98 % of the L X-rays are created by the four γ-transitions shown in Fig. 16. The average coincidence probability of an observed L X-ray, P(LX), is calculated as follows (cf. Eq. 17):

$$P(LX) = p(LX_{26.3})\cdot R_{LX_{26.3}} + p(LX_{33.2})\cdot R_{LX_{33.2}} + p(LX_{43.4})\cdot R_{LX_{43.4}} + p(LX_{59.5})\cdot R_{LX_{59.5}} \qquad (39)$$

where R is the intensity ratio of the L X-ray from a specified conversion to the total L X-rays

$$R_{LX_{26.3}} = \frac{e_{LX_{26.3}}}{e_{LX}} = \frac{e_{26.3}\cdot\alpha_{L26.3}}{\sum_i e_i\cdot\alpha_{Li}} = 0.2035$$

with $\sum_i e_i\cdot\alpha_{Li} = e_{26.3}\cdot\alpha_{L26.3} + e_{33.2}\cdot\alpha_{L33.2} + e_{43.4}\cdot\alpha_{L43.4} + e_{59.5}\cdot\alpha_{L59.5}$

Similarly,

$$R_{LX_{33.2}} = \frac{e_{LX_{33.2}}}{e_{LX}} = 0.2447$$

$$R_{LX_{43.4}} = \frac{e_{LX_{43.4}}}{e_{LX}} = 0.1274$$

$$R_{LX_{59.5}} = \frac{e_{LX_{59.5}}}{e_{LX}} = 0.4244$$

(i) $LX_{26.3}$, L X-rays from the 26.3 keV transition
$LX_{26.3}$ is in cascade with the 43.4 keV and 33.2 keV γ-lines and their associated L X-rays. The coincidence probability of $LX_{26.3}$, $p(LX_{26.3})$, is essentially the same as that of the 26.3 keV γ-line (Eq. 38).

(ii) $LX_{33.2}$, L X-rays from the 33.2 keV transition
$LX_{33.2}$ are in cascade with 43.4 keV, 26.3 keV, and their associated L X-rays

$$p(LX_{33.2}) = p[43.4/LX_{43.4} - \underline{LX_{33.2}}] + p[26.3/LX_{26.3} - \underline{LX_{33.2}}] - p[43.4/LX_{43.4} - 26.3/LX_{26.3} - \underline{LX_{33.2}}] \quad (40)$$

with

$$p[43.4/LX_{43.4} - \underline{LX_{33.2}}] = \frac{e_{43.4}}{e_{33.2}} \cdot a_{26.3} \cdot (a \cdot c)_{33.2} \cdot (\varepsilon_{T43.4} + \alpha_{L43.4} \cdot \bar{\omega}_L \cdot \sum_i k_i \cdot \varepsilon_{T,Li})$$

$$= 0.0002 \ \varepsilon_{T43.4} + 0.0128 \sum_i k_i \cdot \varepsilon_{T,Li} \quad (41)$$

$$p[26.3/LX_{26.3} - \underline{LX_{33.2}}] = \frac{e_{26.3}}{e_{33.2}} \cdot (a \cdot c)_{33.2} \cdot (\varepsilon_{T26.3} + \alpha_{L26.3} \cdot \bar{\omega}_L \cdot \sum_i k_i \cdot \varepsilon_{T,Li})$$

$$= 0.103 \ \varepsilon_{T26.3} + 0.325 \sum_i k_i \cdot \varepsilon_{T,Li} \quad (42)$$

$$p[43.4/LX_{43.4} - 26.3/LX_{26.3} - \underline{LX_{33.2}}]$$

$$= \frac{e_{43.4}}{e_{33.2}} \cdot (a \cdot c)_{26.3} \cdot (a \cdot c)_{33.2} \cdot (\varepsilon_{T43.4} + \alpha_{L43.4} \cdot \bar{\omega}_L \cdot \sum_i k_i \cdot \varepsilon_{T,Li}) \cdot (\varepsilon_{T26.3} + \alpha_{L26.3} \cdot \bar{\omega}_L \cdot \sum_i k_i \cdot \varepsilon_{T,Li})$$

$$= 2 \cdot 10^{-5} \ (\varepsilon_{T43.4} + 65.22 \sum_i k_i \cdot \varepsilon_{T,Li}) \cdot (\varepsilon_{T26.3} + 3.16 \sum_i k_i \cdot \varepsilon_{T,Li}) \quad (43)$$

$$p(LX_{33.2}) = 2\cdot10^{-4}\ \varepsilon_{T43.4} + 0.103\ \varepsilon_{T26.3} + 0.337\ \sum_i k_i\cdot\varepsilon_{T,Li}$$

$$- 2\cdot10^{-5}\ (\varepsilon_{T43.4} + 65.22\ \sum_i k_i\cdot\varepsilon_{T,Li})\cdot(\varepsilon_{T26.3} + 3.16\ \sum_i k_i\cdot\varepsilon_{T,Li}) \quad (44)$$

(iii) $LX_{43.4}$, L X-rays from the 43.4 keV transition

$LX_{43.4}$ is in two cascade chains, one with 59.5 keV and the other with 26.3 and 33.2 keV.

$$p(LX_{43.4}) = p[\underline{LX}_{43.4} - 59.5/LX_{59.5}] + [\underline{LX}_{43.4} - 26.3/LX_{26.3}] + p[\underline{LX}_{43.4} - 33.2/LX_{33.2}] - p[\underline{LX}_{43.4} - 26.3/LX_{26.3} - 33.2/LX_{33.2}] \quad (45)$$

with

$$p[\underline{LX}_{43.4} - 59.5/LX_{59.5}] = (a\cdot c)_{59.5}\cdot(\varepsilon_{T59.5} + \alpha_{L59.5}\cdot\bar{\omega}_L\cdot\sum_i k_i\cdot\varepsilon_{T,Li})$$

$$= 0.435\ \varepsilon_{T59.5} + 0.192\ \sum_i k_i\cdot\varepsilon_{T,Li} \quad (46)$$

$$\bar{p}[\underline{LX}_{43.4} - 26.3/LX_{26.3}] = (a\cdot c)_{26.3}\cdot(\varepsilon_{T26.3} + \alpha_{L26.3}\cdot\omega_L\cdot\sum_i k_i\cdot\varepsilon_{T,Li})$$

$$= 0.007\ \varepsilon_{T26.3} + 0.022\ \sum_i k_i\cdot\varepsilon_{T,Li} \quad (47)$$

$$p[\underline{LX}_{43.4} - 33.2/LX_{33.2}] = a_{26.3}\cdot(a\cdot c)_{33.2}\cdot(\varepsilon_{T33.2} + \alpha_{L33.2}\cdot\bar{\omega}_L\cdot\sum_i k_i\cdot\varepsilon_{T,Li})$$

$$= 3.4\cdot10^{-4}\ \varepsilon_{T33.2} + 0.025\ \sum_i k_i\cdot\varepsilon_{T,Li} \quad (48)$$

$$p[\underline{LX}]_{43.4} - 26.3/LX_{26.3} - 33.2/LX_{33.2}]$$

$$= (a\cdot c)_{26.3}\cdot(a\cdot c)_{33.2}\cdot(\varepsilon_{T26.3}+\alpha_{L26.3}\cdot\bar{\omega}_L\cdot\sum_i k_i\cdot\varepsilon_{T,Li})\cdot(\varepsilon_{T33.2}+\alpha_{L33.2}\cdot\bar{\omega}_L\cdot\sum_i k_i\cdot\varepsilon_{T33.2})$$

$$= 4\cdot10^{-5}\ (\varepsilon_{T26.3} + 3.16\ \sum_i k_i\cdot\varepsilon_{T,Li})\cdot(\varepsilon_{T33.2} + 72.6\ \sum_i k_i\cdot\varepsilon_{T,Li}) \quad (49)$$

So

$$p(LX_{43.4}) = 0.435\ \varepsilon_{T59.5} + 0.007\ \varepsilon_{T26.3} + 3.4\ 10^{-4}\ \varepsilon_{T33.2} + 0.24\ \sum_i k_i\cdot\varepsilon_{T,Li} - 4\cdot10^{-5}\ (\varepsilon_{T26.3} + 3.16\ \sum_i k_i\cdot\varepsilon_{T,Li})\cdot(\varepsilon_{T33.2} + 72.6\ \sum_i k_i\cdot\varepsilon_{T,Li}) \quad (50)$$

(iv) $LX_{59.5}$, L X-rays from the 59.5 keV transition

The coincidence probability of $LX_{59.5}$, p(59.5), is the same as that of the 59.5 keV γ-line (Eq. 32).

Finally, the P(LX) is expressed as the following:

$$P(LX) = 0.2035\ p(LX_{26.3}) + 0.2447\ p(LX_{33.2}) + 0.1274\ p(LX_{43.4}) + 0.4244\ p(LX_{59.5}) \quad (60)$$

and the coincidence correction factor COI(LX) is

$$COI(LX) = 1 - P(LX) \quad (70)$$

Experimental

The ε_p-calibration was carried out for an n-type gamma-X detector (Ortec GMX-model), horizontally mounted with a 0.5 mm beryllium window and 0.3-μm inactive germanium layer. The relative efficiency and energy resolution (FWHM) of the detector for ^{60}Co 1333 keV are 34.8% and 1.77 keV, respectively. The detector was connected to a ND-680 nuclear system through an Ortec spectroscopy amplifier/gated integrator 673 and a ND ADC570. The amplifier time constant was set to 6 μs. The net peak area for γ-lines was calculated using the computer program built into the ND-680 system; the same calculation for multi-energy K X-rays was carried out manually, dealing with the K X-rays as K_α and K_β with their respective effective energies.

Standard radioactive solutions listed in Table 1 were used to prepare 11 radioactive standard γ-ray sources by weighing suitable amounts into half-dram polyethylene containers and then diluting to a volume of 1 cm^3. The activities of the calibration sources were made so as to keep the counting rate (CPS) lower than 400, avoiding pile-up and random coincidence. The uncertainties of the standard radioactive solutions shown in Table 1 vary from 0.5% (^{241}Am) to 4.6% (^{113}Sn). A strong β^--source was prepared in a similar manner from a ^{32}P reference

solution with an uncertainty of 10%. Counting statistics were controlled to be better than 0.5% for most X- and γ-lines measurements, but no poorer than 1% for the rest.

In-house radioactive sources of ^{22}Na, ^{24}Na, ^{51}Cr, and ^{65}Zn were calibrated by measuring at positions far from the detector, where the detector efficiencies were well established by the standard radioactive sources.

P/T-determination

The peak-to-total ratio, $P/T = \varepsilon_p/\varepsilon_T$, serves to obtain the total efficiency ε_T, which is the essential parameter in the calculation of the coincidence factor COI, according to the preceding sections.

The radioactive sources ^{109}Cd (K X-rays, 22.6 keV), ^{241}Am (59.5 keV), ^{57}Co (122.1 keV), ^{203}Hg (279.2 keV), ^{51}Cr (320.1 keV), ^{137}Cs (661.6 keV), ^{54}Mn (834.8 keV), and ^{65}Zn (1115.5 keV) were measured at the 7 positions listed in Table 3. P/T was calculated as the ratio of the net peak area to the total area of the complete γ-spectrum. The latter was compensated for the cut-off of the low-energy part below the threshold energy; the contributions from the environmental background were subtracted along with any co-existing X-rays, γ-rays, and β-particles other than those under consideration. So the P/T-value of 122 keV (^{57}Co) was obtained by applying an iterative method for subtracting the contributions from 14 and 136 keV. The same procedure was applied to the P/T-calculations of the following lines: the 279 keV (^{203}Hg, subtracting the K X-rays contribution), 1115.5 keV (^{65}Zn, subtracting the 511-keV contribution), and 22.6 keV (^{109}Cd, subtracting the 88-keV contribution). When counted at the 4 positions with no perspex β-absorber between the n-type detector and the source (see Table 2), corrections were applied for the contribution from 1173-keV β-particles in the P/T-calculation for 661 keV (^{137}Cs). The effect of the L X-

rays on the P/T-value of 59.5 keV (^{241}Am) was corrected for by simply subtracting the peak-area of the L X-rays. The experimentally determined P/T-curves are shown in Fig. 17.

A reference radioactive source ^{32}P, the pure β^--emitter with maximum energy 1.7 MeV, was measured at the 7 positions to obtain ε_{T,β^-}, the total efficiency of β-rays. ε_{T,β^-} was calculated as follows:

$$\varepsilon_{T,\beta^-} = \frac{N_T}{A_0 \cdot e_\beta \cdot t_m} \tag{71}$$

where N_T - the total counts of the obtained spectrum, corrected for the environmental background

e_β - absolute β^--emission intensity

The results are shown in Table 2.

ε_p-determination

The standard γ-ray sources of 15 nuclides were measured at 7 separate positions with distances to the detector from 0.88 to 17.5 cm, with and without a perspex β-absorber between the detector and sample, as indicated in Table 3. The peak efficiency was then calculated by

$$\varepsilon_p = \frac{N_p}{A_0 \cdot e \cdot t_m \cdot COI} \tag{72}$$

where A_0 - absolute activity

e - emission intensity of measured γ or X-ray

COI - coincidence correction factor (see Eq. 12)

The results are presented in Figs. 18 and 19.

Results and Discussion

P/T curves

Obviously, single-line photon emitters are the nuclides most suitable for determining peak-to-total ratios. For use with an n-type detector, however, the number of such nuclides is quite limited. The nuclides used in this work were selected to satisfy the requirements of uniformly covering a wide energy range, and of being practically coincidence-free when measured close to the detector; they have a single γ-line (^{51}Cr and ^{54}Mn) or at least a dominant one so that the corrections for co-existing X-, γ-, and β-rays will not result in large errors for the P/T values.

Figure 17 shows that as a log-log plot versus photon energy the P/T curves are linear down to about 200 keV; thus a small number of nuclides is sufficient to obtain reliable P/T values in this energy region. At the position closest to the detector (0.88 cm), the uncertainties of the P/T-values in this region varied from 0.75% (^{54}Mn) to 1.6% (^{203}Hg), with the intermediate percentages of 0.83% (^{51}Cr), 1.0% (^{137}Cs) and 1.1% (^{65}Zn).

In the energy region below 200 keV, however, the P/T curves do not appear to have a common shape that could be fitted to the three P/T-values available in this work. At the 0.88 cm position, the uncertainties of the P/T-values found for ^{57}Co, ^{241}Am and ^{109}Cd are 1.1%, 12%, and 7.1%, respectively. The large uncertainty associated with the P/T value of ^{241}Am (59.5 keV) is due mainly to the correction for the L X-rays. It was found that an aluminium absorber (800 mg/cm^2) could totally eliminate the L X-rays, so that no correction was needed; however, the corresponding P/T value is then valid only for the particular geometry with an aluminium absorber - and not for the rest of the work.

The large uncertainty for ^{109}Cd is due mainly to a correction for undefined low-energy photon peaks, probably X-rays excited by the ^{109}Cd in the materials surrounding the detector. Nevertheless, from the point of view of coincidence correction, an uncertainty up to 15% in this energy region is tolerable; this is due to a large error reduction obtained when calculating the COI factor, as discussed in the following paragraph.

COI factors

The coincidence correction factors COI, defined by Eq. (11), were calculated for those photon lines affected by cascade coincidences, based on corresponding formulae in Figs. 2-16. The results are presented in Table 3.

As expected, serious coincidence effects occur at the position closest to the detector (0.88 cm). The 1274.5 keV γ-ray of ^{22}Na is in cascade with the 511-keV annihilation, and shows the strongest coincidence effect. When measuring at the closest position we must correct for a counting loss of 27%. Even at the most distant position, 17.5 cm from the detector and with a 1.0 cm perspex absorber, a coincidence correction of 1.4% should be applied.

The 1.0 cm perspex absorber removed most low-energy photons so that the main γ-lines of ^{57}Co (122.1 keV and 136.5 keV), ^{85}Sr (514 keV), and ^{241}Am (59.5 keV) were coincidence-free even when counted at the 2.70 cm position. In addition, the coincidence effects of the remaining photon lines of ^{241}Am (L X-rays and 26.3 keV γ-line) were mostly reduced.

Coincidence of K X-rays with a γ-line could play an important role as demonstrated by the COI values of the 165.9 keV (^{139}Ce). This line is in cascade with the K X-rays from electron capture (see Fig. 14), and a 12.4% counting loss should be corrected for at the 0.88 cm position. Because of

the relatively high energy of the K X-rays, there was still a 4.7% coincidence effect at the 2.70 cm position with the 1.0 cm perspex absorber.

The coincidence of high-energy β^--particles and their bremsstrahlung should also be taken into acccunt when the n-type detector is used. As shown in Fig. 3, the 1368.6 keV and 2754.0 keV γ-rays from ^{24}Na are in cascade with each other and also with the 1.39 MeV β^--rays. Table 3 shows that at the 0.88 cm position the coincidence effects of these two γ-lines were 11.7% and 13.4%, respectively. The β^--coincidence contributed 15% and 13%, respectively, to the total effects. The β^--coincidence contribution fractions decreased to only 3-4% of the total coincidence effects at the 2.70 cm position, with the 1.0 cm perspex absorber.

The total detection efficiencies for ^{32}P-particles or bremsstrahlung (Table 2) were used for the β^--coincidence calculation of ^{24}Na. Obviously, the ε_{T,β^-} is a function of the β^--energy spectrum. The difference in the energies of ^{32}P (1.7 MeV) and ^{24}Na (1.4 MeV) would introduce some error in the COI calculation, but it was presumed to be unimportant due to the large error reduction in the calculation of COI.

As a demonstration, we will discuss uncertainties of the COI values at the 0.88 cm position for some representative photon lines. A relative uncertainty of 1.2% was found in the COI value (0.729) of ^{22}Na 1274.5 keV, mainly coming from the uncertainty of $\varepsilon_{T,511}$. The uncertainties associated with the nuclear constants used in the calculation formulae (ω, e_γ, a, and α) may be neglected for most nuclides in this work, because their decay schemes and nuclear parameters are well established. In this example, an uncertainty of about 3% in $\varepsilon_{T,511}$ resulted in an uncertainty of only 1.2% in the COI value due to the large error reduction, as shown next:

In the simplest case of γ–γ coincidence

COI = 1–P (see Eq. (12), $^{SUM}P = 0$), and
$P = a \cdot c \cdot \varepsilon_T$ (see Eq. (2)).

If uncertainties of the nuclear constants a and c are ignored, the relative uncertainty of COI is

$$S_{COI} = \frac{S_{\varepsilon_T}}{1/P - 1} \qquad (73)$$

In general, the largest value of P is about 0.25 (closest position to a large volume detector), and the uncertainty of ε_T will be reduced by a factor of three. In this work most P values at the 0.88 cm position are about 0.15 or lower; the error reduction factors are then 5.6 or higher. In other words, a 10% uncertainty of the ε_T will result in uncertainties of less than 2% for the calculated COI values.

As an example of X–γ coincidence, the uncertainty in the COI value (0.876) of the 165.9 keV (^{139}Ce) was found to be 2.1%; it stems from the uncertainties of $\varepsilon_{T,Kx}$ and atomic parameters related to X-ray emission. The latter numbers, particular the ω, have larger uncertainties.

For the γ–γ coincidence in the energy region higher than 200 keV, where both ε_p and P/T were well determined, the COI values were established with uncertainties below about 1%. For example the relative uncertainty in the COI value (0.880) for ^{60}Co 1332 keV was 0.5%.

As discussed above, 1368 keV of ^{24}Na is in cascade with the 1.4 MeV β^-- and 2754 keV γ-lines. The uncertainty in the COI value (0.883) of the 1368 keV was found to be 1.1 %, estimated from the uncertainties of $\varepsilon_{T,2754}$ (5.8 %) and ε_{T,β^-} (20 %).

This example clearly shows that a significant coincidence effect can be corrected for satisfactorily, in spite of large uncertainties associated with the ε_T-values.

ε_p-curves

Figures 18 and 19 show photo-peak efficiencies ε_p calculated by Eq. (71) using coincidence correction factors listed in Table 3 for two counting geometries: without and with a 1.0 cm perspex absorber, respectively. The ε_p has a maximum value at the region 60-90 keV (without absorber) or 60-100 keV (with the absorber). In a log/log representation, ε_p is a linear function of photon energy E in the energy region from about 200 keV to 2000 keV. Above 2000 keV, ε_p at the 2754.0 keV point (^{24}Na) indicates a more rapid decrease, corresponding to an increasing escape peak efficiency. In the energy region below 50 keV, ε_p decreases with decreasing photon energy due to the self-absorption in the sample volume together with the absorption in the air, the beryllium window, and the 0.3 μm inactive germanium layer. For the counting geometry with 1.0 cm perspex absorber, the decrease is expected to be much more pronounced.

The uncertainty evaluation of the ε_p-values in Figs. 18 and 19 should be based on Eq. (72). It should include the uncertainties of the absolute photon emission intensities of the standard sources listed in Table 1, counting statistics of the net peak area, and the COI factor. For homemade sources that were calibrated by measuring at positions furthest from the detector, the uncertainty evaluation should include also the uncertainties associated with the calibration procedure. For the main γ-lines evaluated in this work, the uncertainties of photon emission intensities are negligible. But this is not the case with weak γ-lines and X-rays. For instance, the uncertainties of the 14.4 (^{57}Co) and 36.6 keV (K_β, ^{137}Cs) lines are 2.6% and 3.7%, respectively.

The uncertainties of the ε_p-values at 17.5 cm positions with and without the 1.0 cm perspex absorber were largely determined by the uncertainties of the standard radioactive sources. There were no or only minor coincidence effects. The uncertainties were estimated to be 2.0% in the region 200-2000 keV, 2.1% for the 2754.0 keV point (^{24}Na), 3.2% in the 50-200 keV region and 3.8% for energies below 50 keV.

The uncertainty of the coincidence correction should be taken into account for uncertainty evaluations of ε_p-values at positions other than 17.5 cm. For the ε_p-values at the 0.88 cm position, where the largest coincidence corrections were applied, the uncertainties were estimated to be 2.8% in the 200-2000 keV region, 3.1 % for the ε_p-value at 2754 keV, 3.8 % in the 50-200 keV region and 4.3 % for the region below 50 keV.

Conclusion

This work successfully demonstrates a method to determine the photo-peak efficiency of the n-type gamma-X detector at positions close to the detector, for the energy range 12 to 2754 keV. Between 200 and 2000 keV, uncertainties are only a few per cent and for the other energies no more than 5%. The key to achieving these results was to correct accurately for the coincidence effects using formulae derived in this work for γ-γ, X-γ, γ-511-keV annihilation, and β-γ cascade coincidences. Additional work was required to determine the P/T-curves with a small number of nuclides.

References

[1] Moens, L., De Donder, J., Lin, X.L., De Corte, F., and Hoste, J., Nucl. Instrum. and Methods, 187 (1981) 451

[2] Moens, L., Ph.D. Thesis, State Univ. Gent (1981)

[3] Lin, X.L. and Zhang, W.H., Nucl. Tech. 10 (1986) 1

[4] De Corte, F., "Hoger Aggregaat" Thesis, State Univ. Gent (1987)

[5] Lagoutine, F., Coursol, N., and Legrand, J., Table de Radionucleides, CEA-LMRI, Saclay (1982, 1983 and 1984)

[6] Brown, E. and Firestone, R., Table of Radioactive Isotopes (Ed. Shirley, V.S.), John Wiley & Sons, New York (1986)

[7] Lederer, C.M. and Shirley, V.S., Table of Isotopes, 7th Edit., John Wiley & Sons, New York (1978)

[8] Ellis-Akovali, Y.A., Nucl. Dat. Sheets 44 (1985) 407

[9] Krause, M.O., Nestor, C.W., Sparks, C.J., and Ricci, E., Oak Ridge Nat. Lab. Report ORNL-5399 (1978)

[10] Gunnink, R., Evans, J.E., and Prindle, A.L. UCRL-52139 (1976)

[11] Yoshizawa, Y., Iwata, Y., Fukuhara, K., and Inoue, H., in: A.L. Nichols, Intern. Committee for Radionuclide Metrology, Rept. ICRM 3nd 2/85 (June 1985)

[12] Schötzig, U. and Schrader, H., Halbwertszeiten und Photonen-Emissionswahrscheinlichkeiten von häufig verwendeten Radionukliden, CPTB-Bericht RA-16 (1984)

[13] Ballaux, C., Coursey, B.M., and Hopper, D.D., Appl. Radiat. Isot. 39 (1988) 1131 (Int. J. Radiat. Appl. Instrum. Part A)

Tables

Table 1 Standard and Reference Radioactive Solutions Used in ε_p-Determination

Table 2 Total Efficiency of ^{32}P β^--rays

Table 3 Coincidence Correction Factor, COI, at Different Counting Conditions

Table 1

Standard/Reference Radioactive Solutions Used in ε_p-Determination

	Nuclide	E_γ keV	Overall Uncertainty %
Certified radioactive solution QCY.44 Amersham (UK)	^{109}Cd	88.1	± 3.8
	^{57}Co	122.1	± 2.3
	^{139}Ce	165.9	± 3.8
	^{203}Hg	279.2	± 2.2
	^{113}Sn	391.7	± 4.6
	^{85}Sr	514.0	± 1.9
	^{137}Cs	661.6	± 3.1
	^{88}Y	898.0	± 3.8
	^{60}Co	1173.2	± 0.8
		1332.6	± 0.8
	^{88}Y	1836.1	± 2.8
Standard radioactive solution - CUZ.64 Amersham (UK)	^{109}Cd	88.1	± 1.17 1.00
Certified radioactive solution Amersham (UK)	^{241}Am	59.5	± 0.5
Certified radioactive solution LMRI (France)	^{54}Mn	834.8	± 1.0
Reference radioactive solution	^{32}P	β^-	± 10 %

Table 2

Total Efficiency of ^{32}P β^--rays

Distance from	without perspex absorber				with a 1.0 cm perspex absorber		
detector face	0.88 cm	2.70 cm	7.60 cm	17.5 cm	2.70 cm	7.60 cm	17.5 cm
ε_{T,β^-} (^{32}P)	1.78×10^{-2}	9.37×10^{-3}	2.51×10^{-3}	5.93×10^{-4}	2.17×10^{-3}	6.30×10^{-4}	1.61×10^{-4}

Table 3

Coincidence Correction Factor, COI, at Different Counting Conditions

Isotope	Photon energy (keV)	COI without perspex absorber				COI with a 1.0 cm perspex absorber between detector and source		
		0.88 cm*	2.70 cm*	7.60 cm*	17.5 cm*	2.70 cm*	7.60 cm*	17.5 cm*
^{22}Na	511.0	0.882	0.940	0.981	0.993	0.942	0.981	0.994
	1274.5	0.729	0.865	0.957	0.986	0.871	0.959	0.986
^{24}Na	1368.6	0.883	0.942	0.981	0.994	0.948	0.983	0.994
	2754.0	0.866	0.933	0.978	0.993	0.940	0.980	0.994
^{57}Co	14.4	0.796	0.900	0.969	0.991	0.908	0.971	0.992
	122.1	0.993	1.0	1.0	1.0	1.0	1.0	1.0
	136.5	1.044	1.022	1.006	1.0	1.0	1.0	1.0
^{85}Sr	13.6	0.852	0.926	0.976	0.992	0.929	0.977	0.993
	514.0	0.968	0.982	0.994	1.0	1.0	1.0	1.0
^{88}Y	898.0	0.859	0.925	0.976	0.992	0.943	0.981	0.994
	1836.1	0.845	0.919	0.974	0.992	0.937	0.980	0.993
^{60}Co	1173.2	0.884	0.941	0.981	0.994	0.943	0.981	0.994
	1332.5	0.880	0.939	0.980	0.993	0.941	0.981	0.994
^{139}Ce	165.9	0.876	0.937	0.983	1.0	0.953	0.987	1.0
^{241}Am	11.87							
	13.93	0.963	0.982	1.0	1.0	0.989	1.0	1.0
	**17.58							
	21.0							
	26.3	0.963	0.981	1.0	1.0	0.993	1.0	1.0
	59.5	0.995	1.0	1.0	1.0	1.0	1.0	1.0

*Distance from the detector face

**Effective energy of L_η and L_β

Figures

Fig. 1. Four basic cascade-decay schemes used for deriving coincidence correction factors

Fig. 2. Decay scheme of ^{22}Na

Fig. 3. Decay scheme of ^{24}Na

Fig. 4. Decay scheme of ^{51}Cr

Fig. 5. Decay scheme of ^{54}Mn

Fig. 6. Decay scheme of ^{57}Co

Fig. 7. Decay scheme of ^{60}Co

Fig. 8. Decay scheme of ^{65}Zn

Fig. 9. Decay scheme of ^{85}Sr

Fig. 10. Decay scheme of ^{88}Y

Fig. 11. Decay scheme of ^{109}Cd

Fig. 12. Decay scheme of ^{113}Sn

Fig. 13. Decay scheme of ^{137}Cs

Fig. 14. Decay scheme of ^{139}Ce

Fig. 15. Decay scheme of ^{203}Hg

Fig. 16. Decay scheme of ^{241}Am

Fig. 17. P/T-curves
a) P/T-curves at 3 positions with a 10-mm perspex absorber
b) P/T-curves at 4 positions without perspex absorber
* distances from the detector face (refer to Table 3)

Fig. 18. ε_p-curves determined at 3 positions with a 10-mm perspex absorber
* distances from the detector face (refer to Table 3)

Fig. 19. ε_p-curves determined at 4 positions without perspex absorber
* distances from the detector face (refer to Table 3)

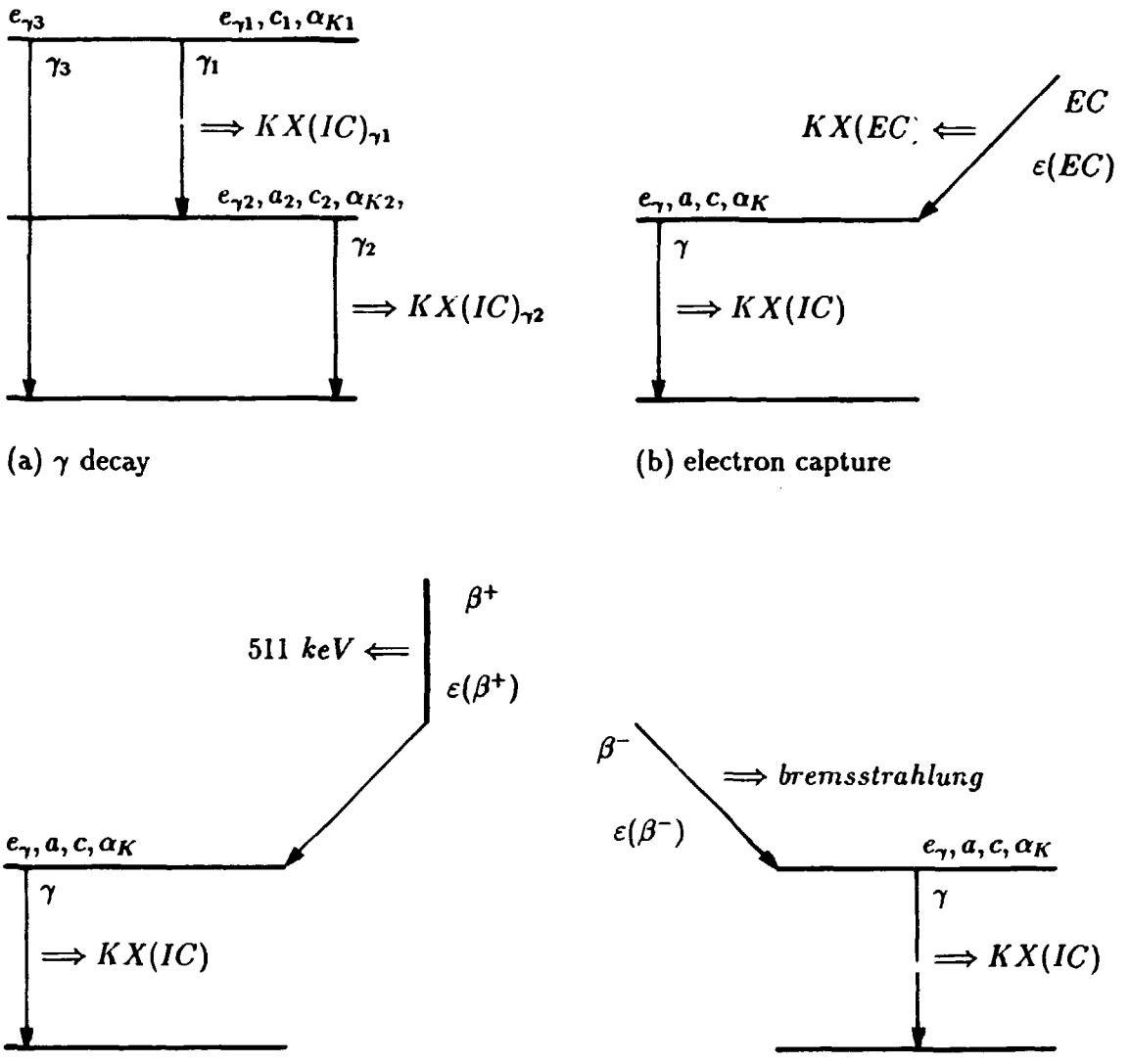

(a) γ decay

(b) electron capture

(c) β^+ decay

(d) β^- decay

Fig. 1. Four basic cascade-decay schemes used for deriving coincidence correction factors.

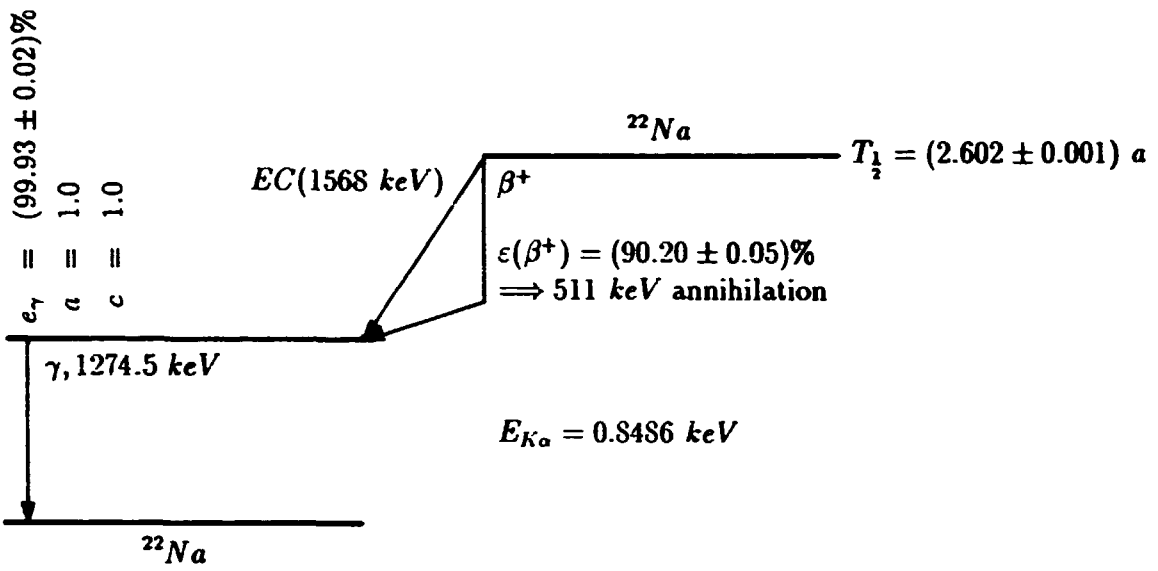

$$COI = 1 - P$$

$$P(1274.5\ keV) = \frac{2\varepsilon(\beta^+)}{e_\gamma} \cdot a \cdot c \cdot \varepsilon_{T,511} = 1.805\ \varepsilon_{T,511}$$

$$P(511\ keV) = a \cdot c \cdot \varepsilon_{T,1274.5} = \varepsilon_{T,1274.5}$$

Fig. 2. Decay scheme of ^{22}Na.

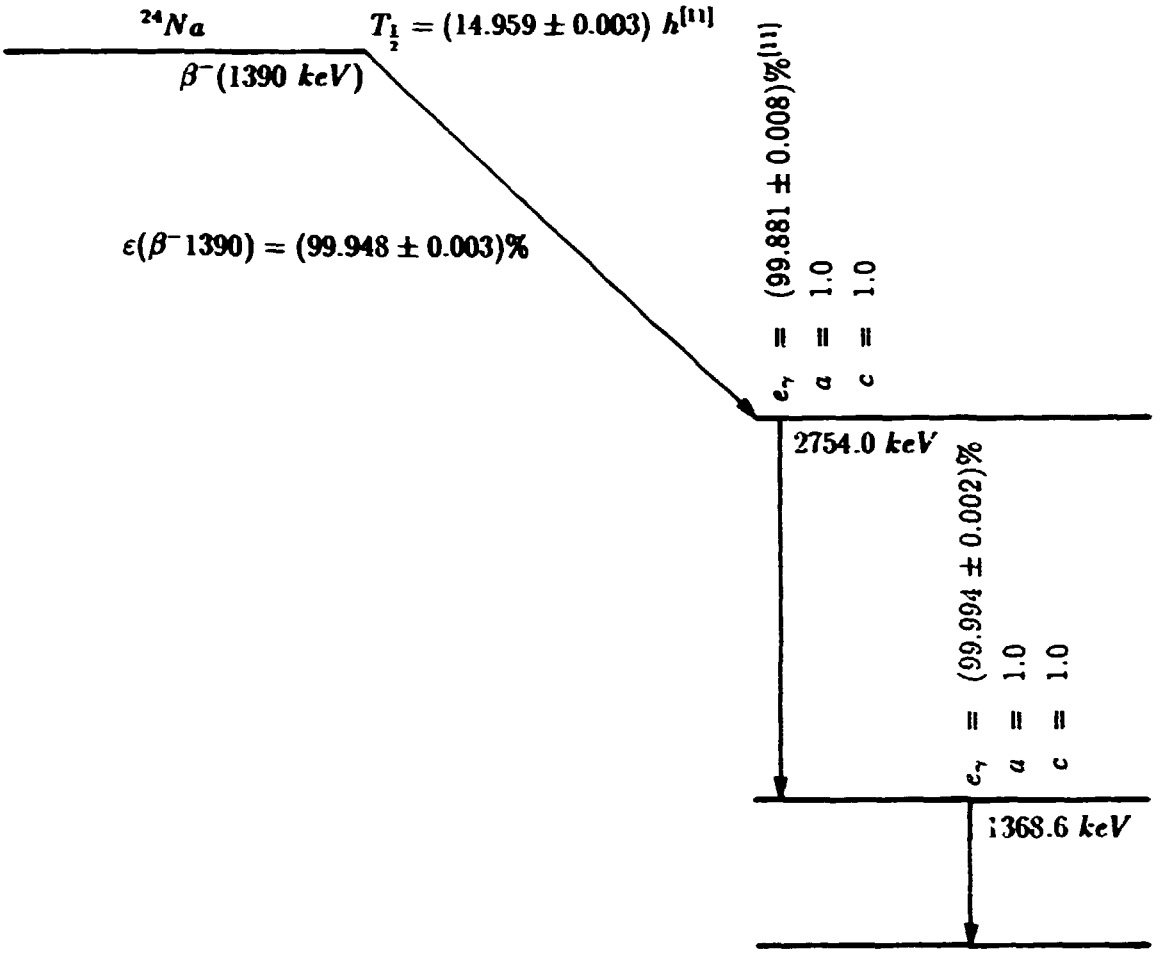

$$COI = 1 - P$$

$$P(1368.6\ keV) = \frac{\varepsilon(\beta^-1390)}{\varepsilon_{1368.6}} \cdot a_{2754.0} \cdot (a \cdot c)_{1368.6} \cdot \varepsilon_{T,\beta^-1390} + \frac{\varepsilon_{2754.0}}{\varepsilon_{1368.6}} \cdot (a \cdot c)_{1368.6} \cdot \varepsilon_{T,2754.0}$$

$$- \frac{\varepsilon(\beta^-1390)}{\varepsilon_{1368.6}} \cdot (a \cdot c)_{2754.0} \cdot (a \cdot c)_{1368.6} \cdot \varepsilon_{T,\beta^-1390} \cdot \varepsilon_{T,2754.0}$$

$$= 0.9995\varepsilon_{T,\beta^-1390}(1 - \varepsilon_{T,2754.0}) + 0.9989\varepsilon_{T,2754.0}$$

$$P(2754.0\ keV) = \frac{\varepsilon(\beta^-1390)}{\varepsilon_{2754.0}} \cdot (a \cdot c)_{2754.0} \cdot \varepsilon_{T,\beta^-1390} + (a \cdot c)_{1368.6} \cdot \varepsilon_{T,1368.6}$$

$$- \frac{\varepsilon(\beta^-1390)}{\varepsilon_{2754.0}} \cdot (a \cdot c)_{2754.0} \cdot (a \cdot c)_{1368.6} \cdot \varepsilon_{T,\beta^-1390} \cdot \varepsilon_{T,1368.6}$$

$$= 1.0007\varepsilon_{T,\beta^-1390}(1 - \varepsilon_{T,1368.6}) + \varepsilon_{T,1368.6}$$

Fig. 3. Decay scheme of ^{24}Na.

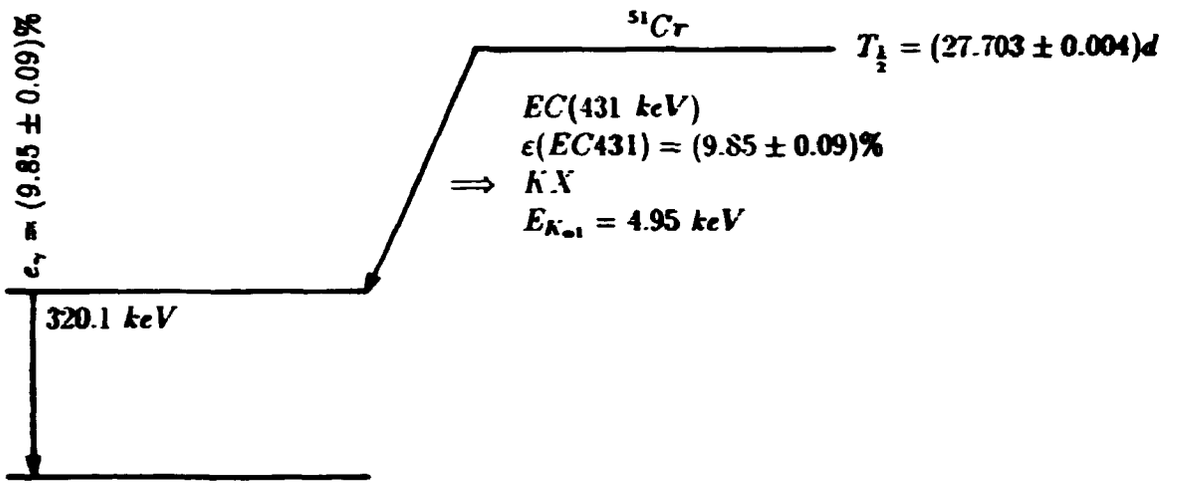

Fig. 4. Decay scheme of ^{51}Cr.

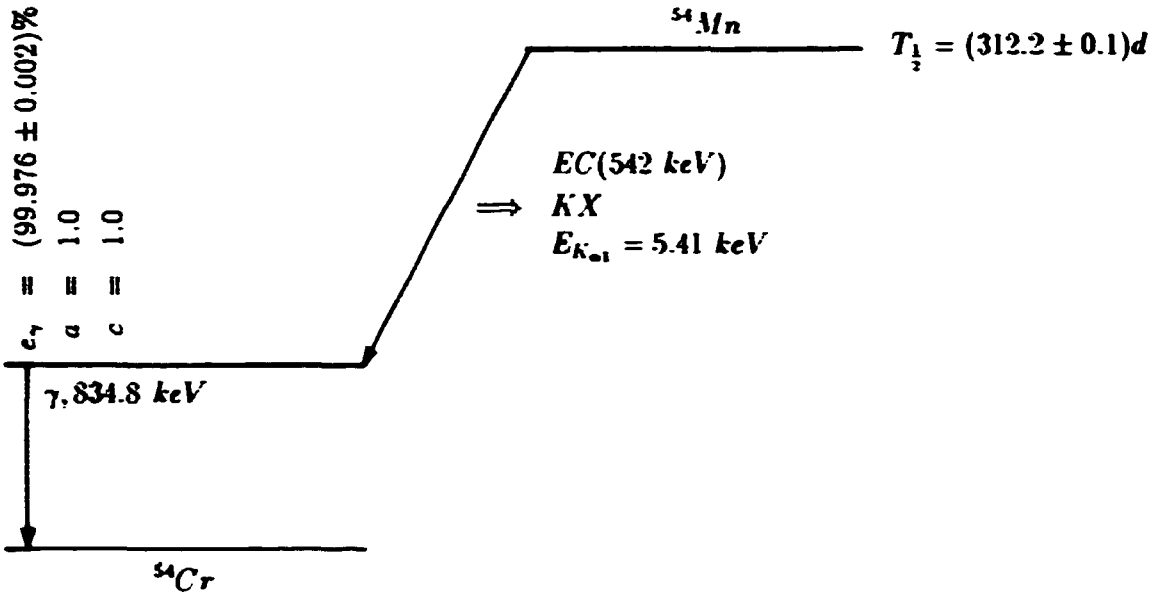

Fig. 5. Decay scheme of ^{54}Mn.

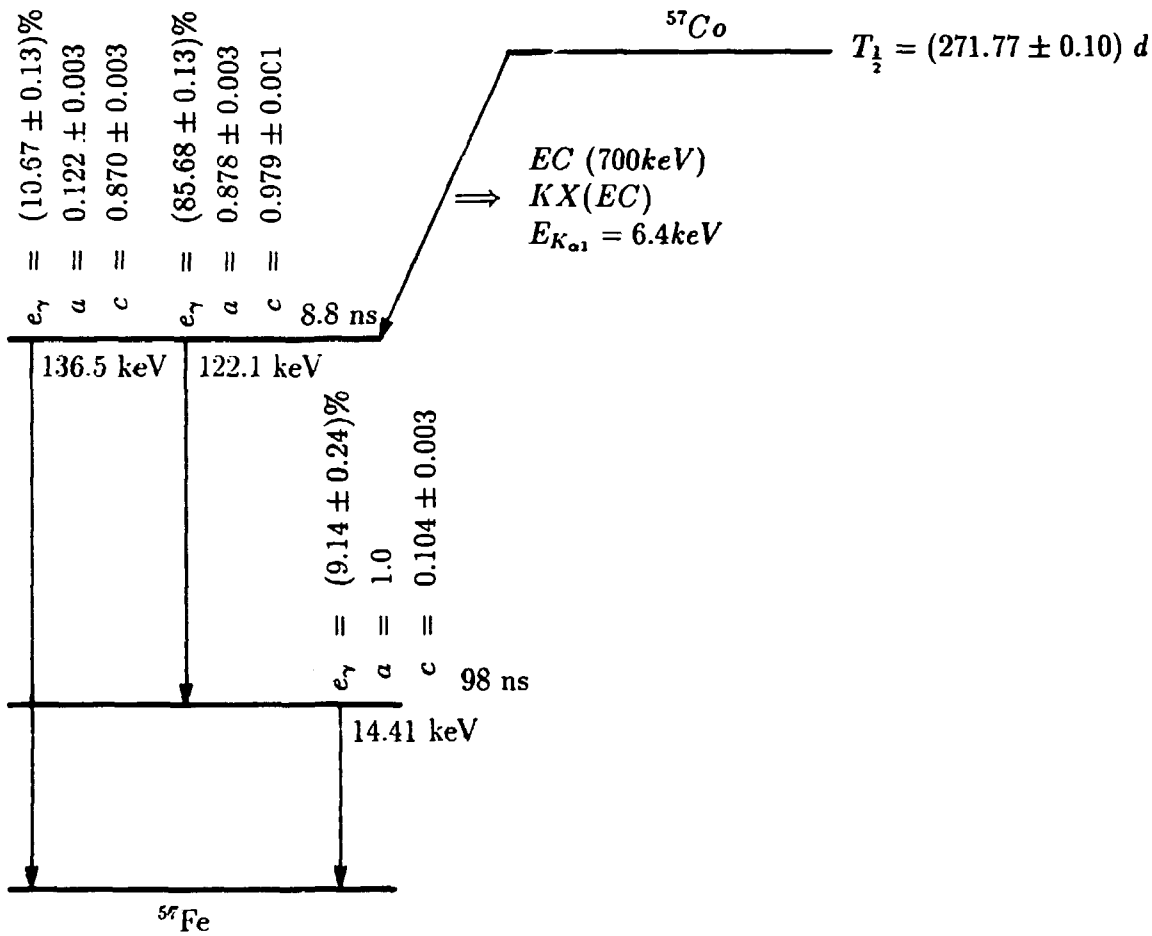

$$COI = 1 + P^{SUM}$$

$$P^{SUM}(136.5keV) = \frac{e_{122.1}}{e_{136.5}} \cdot (a \cdot c)_{14.41} \cdot \frac{\varepsilon_{p,122.1} \cdot \varepsilon_{p,14.41}}{\varepsilon_{p,136.5}} = 0.8351 \frac{\varepsilon_{p,122.1} \cdot \varepsilon_{p,14.41}}{\varepsilon_{\gamma,136.5}}$$

$$COI = 1 - P$$

$$P(122.1\ keV) = (a \cdot c)_{14.41} \cdot \varepsilon_{T,14.41} = 0.104 \varepsilon_{T,14.41}$$

$$P(14.41\ keV) = \frac{e_{122.1}}{e_{14.41}} (a \cdot c)_{14.41} \cdot \varepsilon_{T,122.1} = 0.9749 \varepsilon_{T,122.1}$$

Fig. 6. Decay scheme of ^{57}Co.

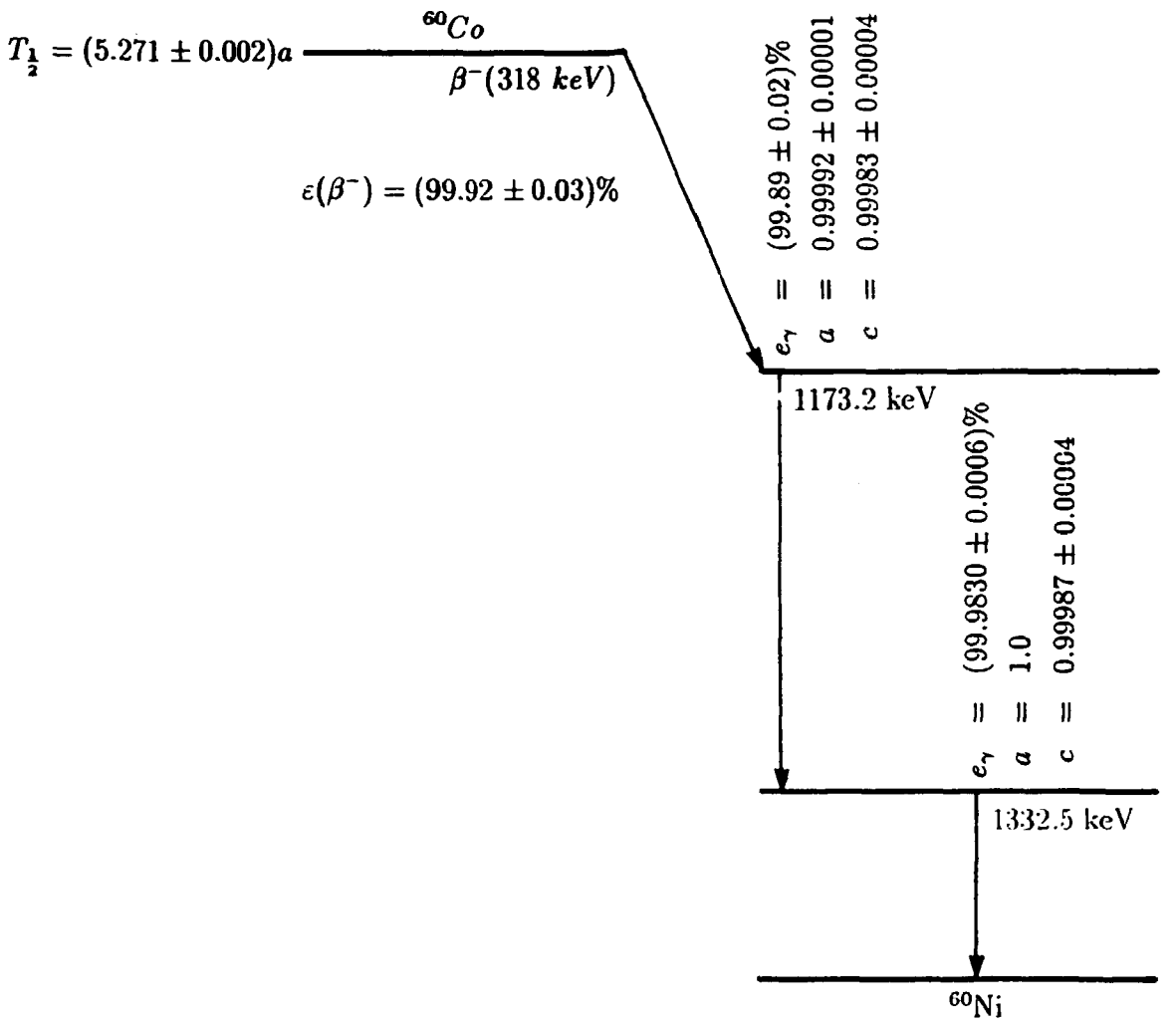

$$COI = 1 - P$$

$$P(1173.2\ keV) = (a \cdot c)_{1332.5} \cdot \varepsilon_{T,1332.5} = 0.9999\varepsilon_{T,1332.5}$$

$$P(1332.5\ keV) = \frac{e_{1173.2}}{e_{1332.5}} \cdot (a \cdot c)_{1332.5} \cdot \varepsilon_{T,1173.2} = 0.9989\varepsilon_{T,1173.2}$$

Fig. 7. Decay scheme of ^{60}Co.

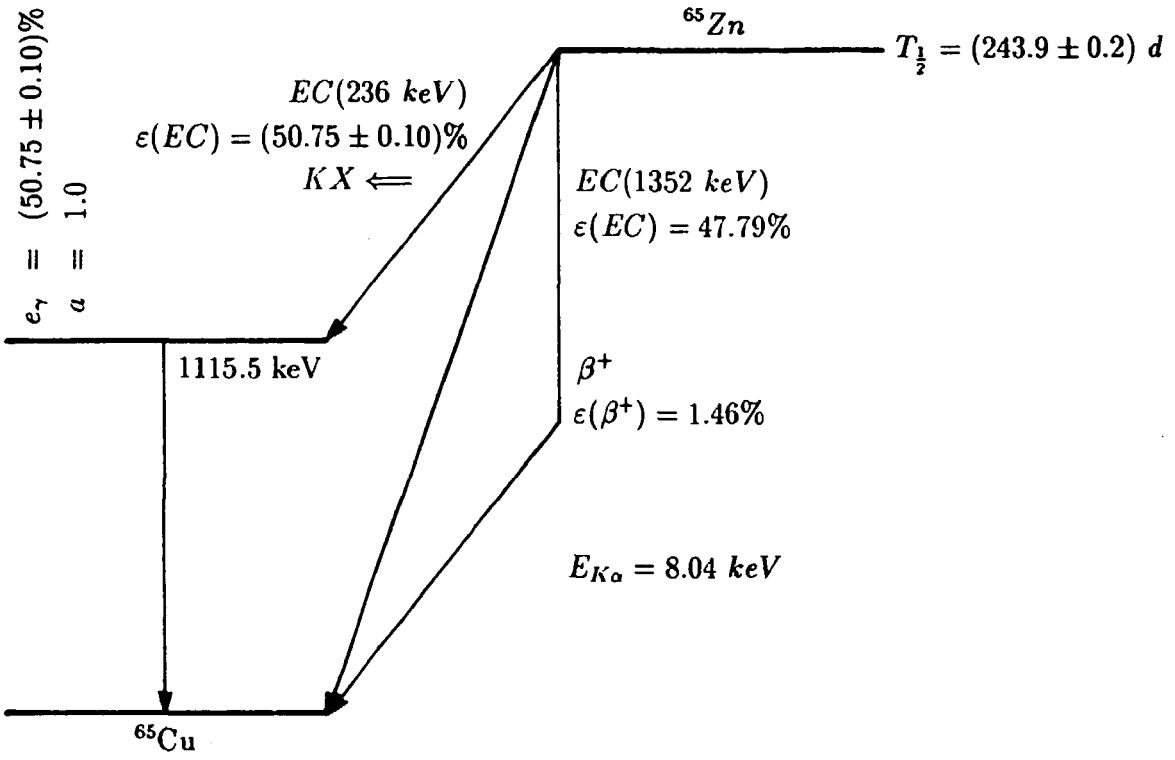

Fig. 8. Decay scheme of ^{65}Zn.

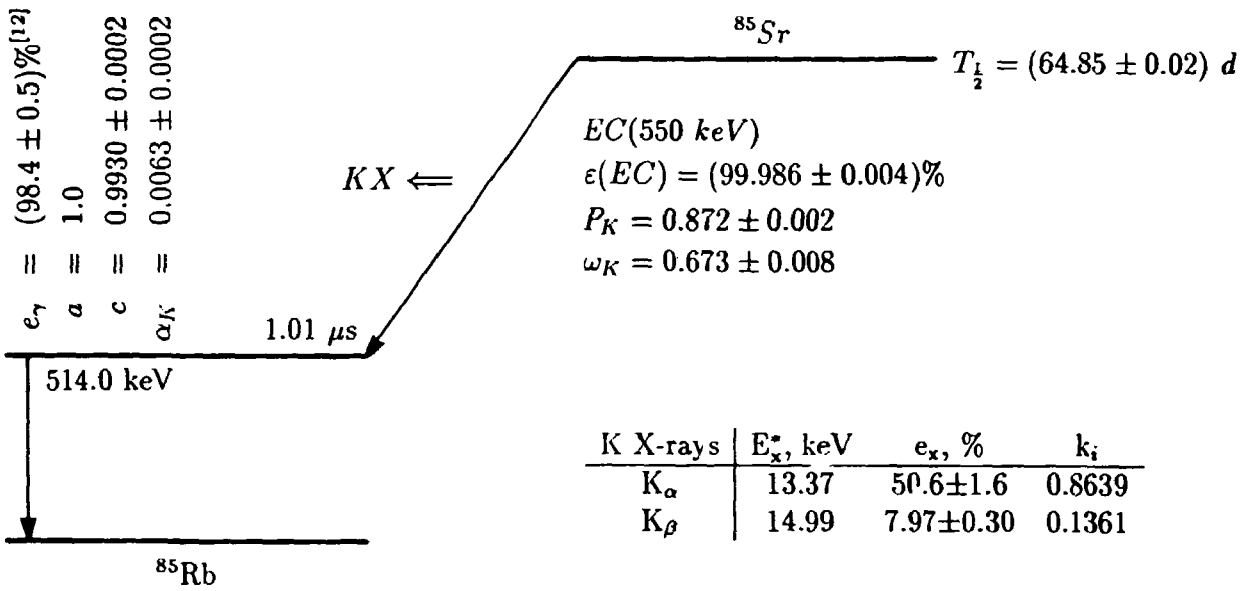

K X-rays	E_x^*, keV	e_x, %	k_i
K_α	13.37	50.6±1.6	0.8639
K_β	14.99	7.97±0.30	0.1361

$$E_x^* = \frac{\sum_i e_{x_i} \cdot E_{x_i}}{\sum_i e_{x_i}}\ ,\ \text{effective energy}$$

where e_{x_i} - emission intensity of E_{x_i}

$$COI = 1 - P$$

$$P(514.0\ keV) = \frac{\varepsilon(EC) \cdot P_K \cdot \omega_K}{e_{514.0}} \cdot a \cdot c \cdot \sum_i k_i \cdot \varepsilon_{T,K_i} = 0.512\varepsilon_{T,13.37} + 0.081\varepsilon_{T,14.99}$$

$$P(K\ \text{X-rays}) = a \cdot c \cdot \varepsilon_{T,514.0} = 0.993\varepsilon_{T,514.0}$$

Fig. 9. Decay scheme of ^{85}Sr.

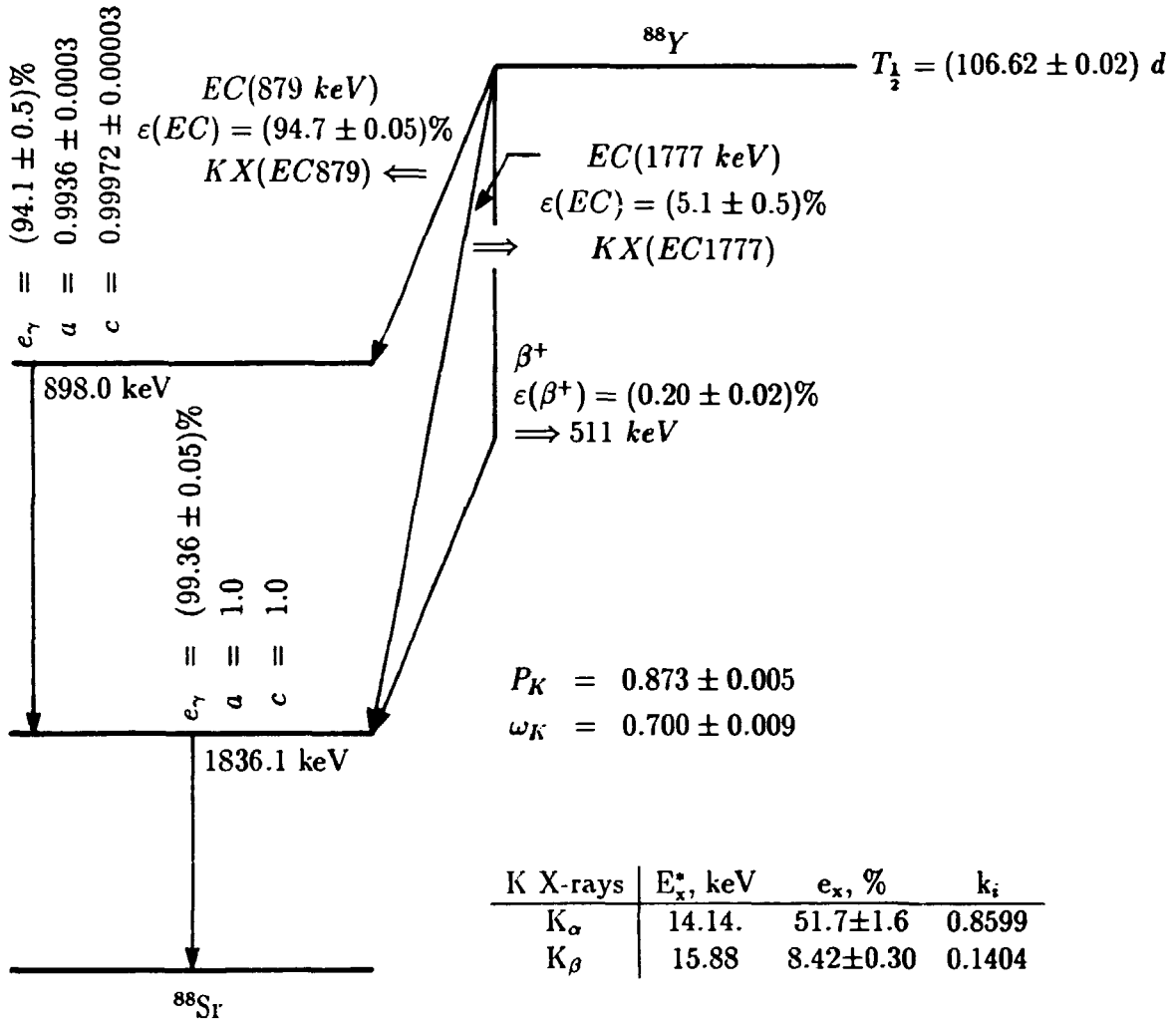

K X-rays	E_x^*, keV	e_x, %	k_i
K_α	14.14.	51.7±1.6	0.8599
K_β	15.88	8.42±0.30	0.1404

$$COI = 1 - P$$

$$P(898.0\ keV)^\dagger = (0.5253\varepsilon_{T,14.14} + 0.0856\varepsilon_{T,15.88}) \cdot (1 - \varepsilon_{T,1836.1}) + \varepsilon_{T,1836.1}$$

$$P(1836.1\ keV)^\dagger = (0.6101 - 0.5786\varepsilon_{T,898.0}) \cdot (0.8599\varepsilon_{T,14.14} + 0.1401\varepsilon_{T,15.88}) + 0.9471\varepsilon_{T,898.0}$$

$$P(K\ \text{X-rays})^\dagger = 0.9425\varepsilon_{T,898.0} \cdot (1 - \varepsilon_{T,1836.1}) + 0.9939\varepsilon_{T,1836.1}$$

† refer to the text for detailed discussion

Fig. 10. Decay scheme of ^{88}Y.

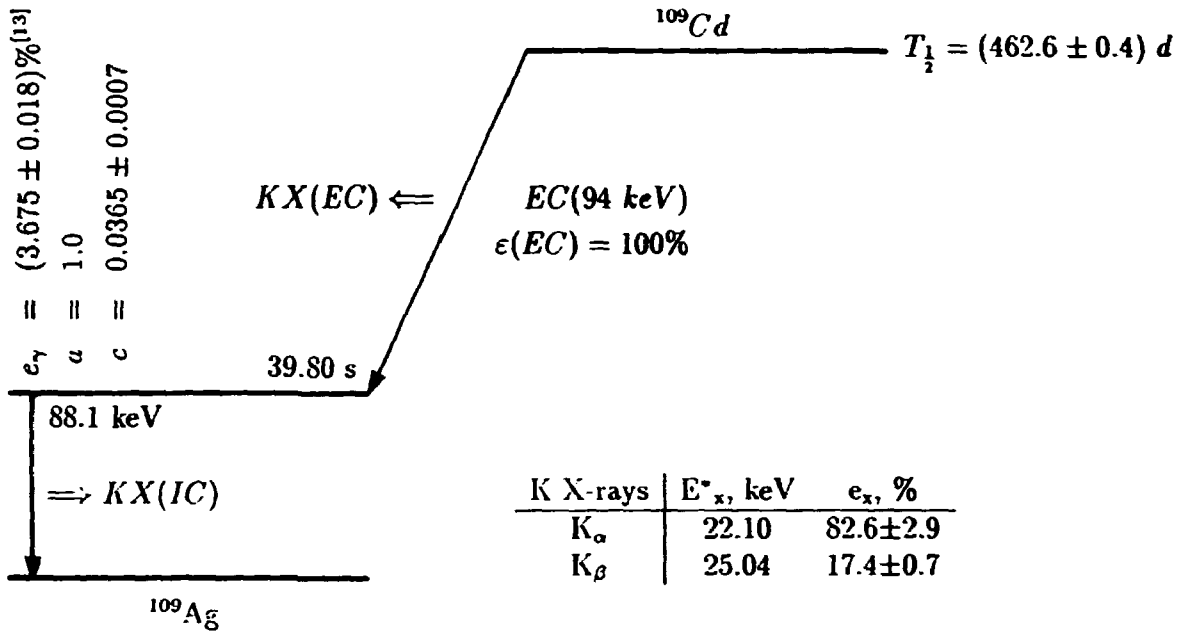

K X-rays	E^*_x, keV	e_x, %
K_α	22.10	82.6±2.9
K_β	25.04	17.4±0.7

Fig. 11. Decay scheme of ^{109}Cd.

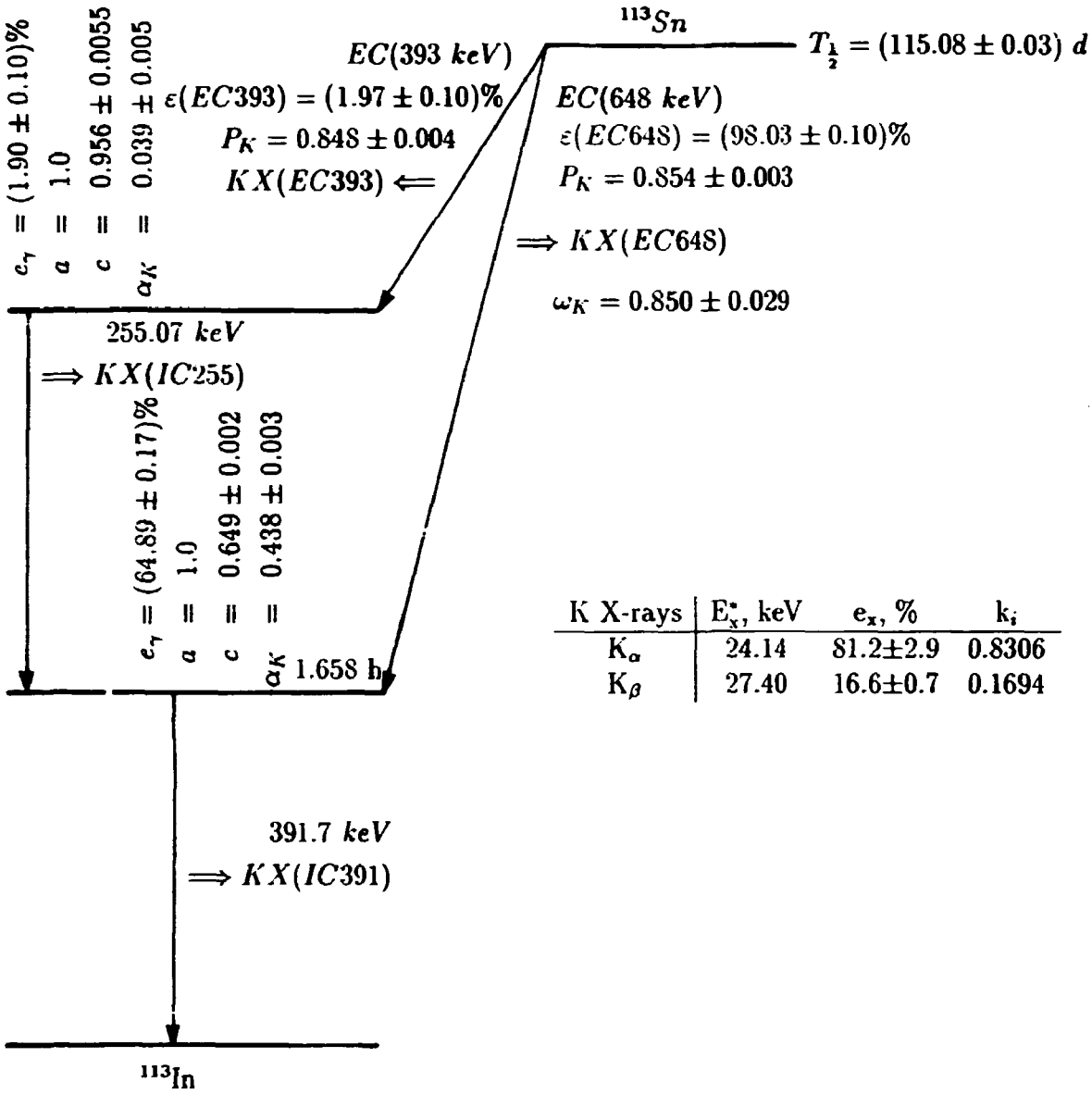

K X-rays	E_x^*, keV	e_x, %	k_i
K_α	24.14	81.2±2.9	0.8306
K_β	27.40	16.6±0.7	0.1694

$$COI = 1 - P$$

$$P(255.07\ keV) = \frac{\varepsilon(EC393) \cdot P_{K393} \cdot \omega_K}{e_{255.07}} \cdot (a \cdot c)_{255.07} \cdot (k_\alpha \cdot \varepsilon_{T,K\alpha} + k_\beta \cdot \varepsilon_{T,K\beta})$$

$$= 0.5934\varepsilon_{T,24.14} + 0.1210\varepsilon_{T,27.40}$$

$$P(K\ \text{X-rays}) = 0.0141\varepsilon_{T,255.1} + 0.0008\varepsilon_{T,24.14} + 0.0002\varepsilon_{T,27.40}$$

Fig. 12. Decay scheme of ^{113}Sn.

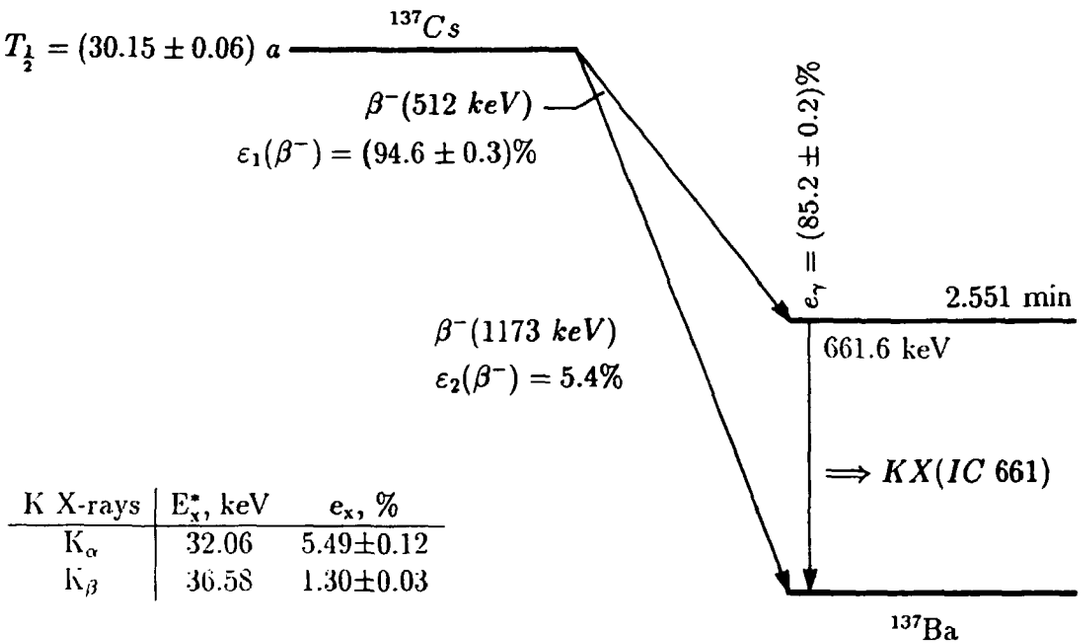

K X-rays	E_x^*, keV	e_x, %
K_α	32.06	5.49±0.12
K_β	36.58	1.30±0.03

Fig. 13. Decay scheme of ^{137}Cs.

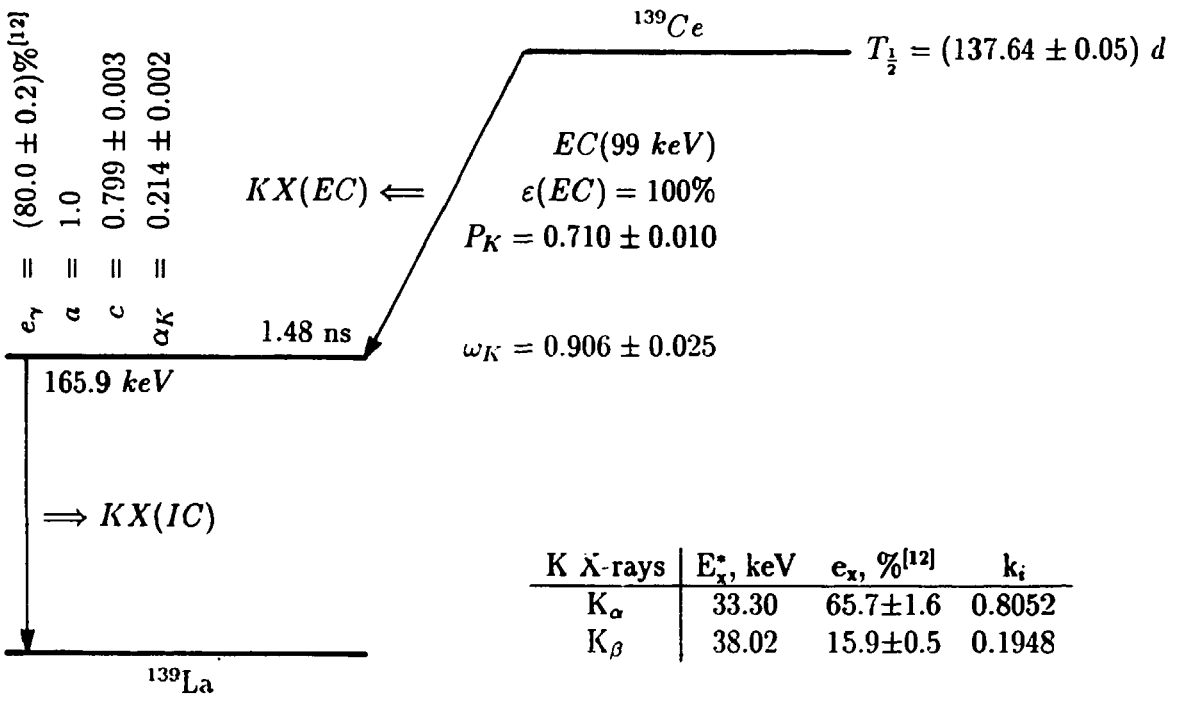

K X-rays	E_x^*, keV	e_x, %[12]	k_i
K_α	33.30	65.7±1.6	0.8052
K_β	38.02	15.9±0.5	0.1948

$$COI = 1 - P$$

$$P(165.9\ keV) = \frac{\varepsilon(EC) \cdot P_K \cdot \omega_K}{e_{165.9}} \cdot (a \cdot c)_{165.9} \cdot (k_\alpha \cdot \varepsilon_{T,k\alpha} + k_\beta \cdot \varepsilon_{T,K\beta})$$

$$= 0.5173\varepsilon_{T,33.30} + 0.1252\varepsilon_{T,38.02}$$

$$P(K\ \text{X-rays}) = R_{KX(EC)} \cdot (a \cdot c)_{165.9}[\varepsilon_{T,165.9} + \alpha_K \cdot \omega_K \cdot (k_\alpha \cdot \varepsilon_{T,K\alpha} + k_\beta \cdot \varepsilon_{T,K\beta})]$$

$$+R_{KX(IC)} \cdot \frac{\varepsilon(EC) \cdot P_K \cdot \omega_K}{e_{165.9}} \cdot (a \cdot c)_{165.9} \cdot (k_\alpha \cdot \varepsilon_{T,K\alpha} + k_\beta \cdot \varepsilon_{T,K\beta})$$

$$= 0.6438\varepsilon_{T,165.9} + 0.2010\varepsilon_{T,33.3} + 0.0486\varepsilon_{T,38.02}$$

$$\text{with } R_{KX(EC)} = \frac{e_{KX(EC)}}{e_{KX(EC)} + e_{KX(IC)}} = 0.8057; R_{KX(IC)} = \frac{e_{KX(IC)}}{e_{KX(EC)} + e_{KX(IC)}} = 0.1943$$

Fig. 14. Decay scheme of ^{139}Ce.

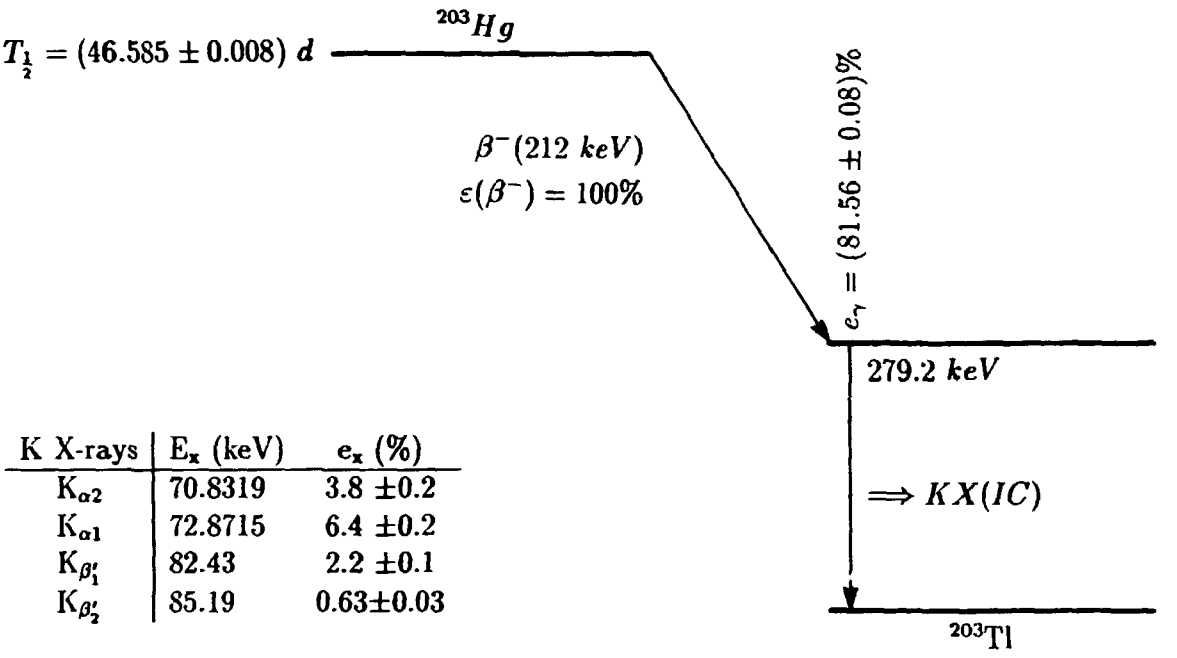

K X-rays	E_x (keV)	e_x (%)
$K_{\alpha 2}$	70.8319	3.8 ±0.2
$K_{\alpha 1}$	72.8715	6.4 ±0.2
$K_{\beta_1'}$	82.43	2.2 ±0.1
$K_{\beta_2'}$	85.19	0.63±0.03

Fig. 15. Decay scheme of ^{203}Hg.

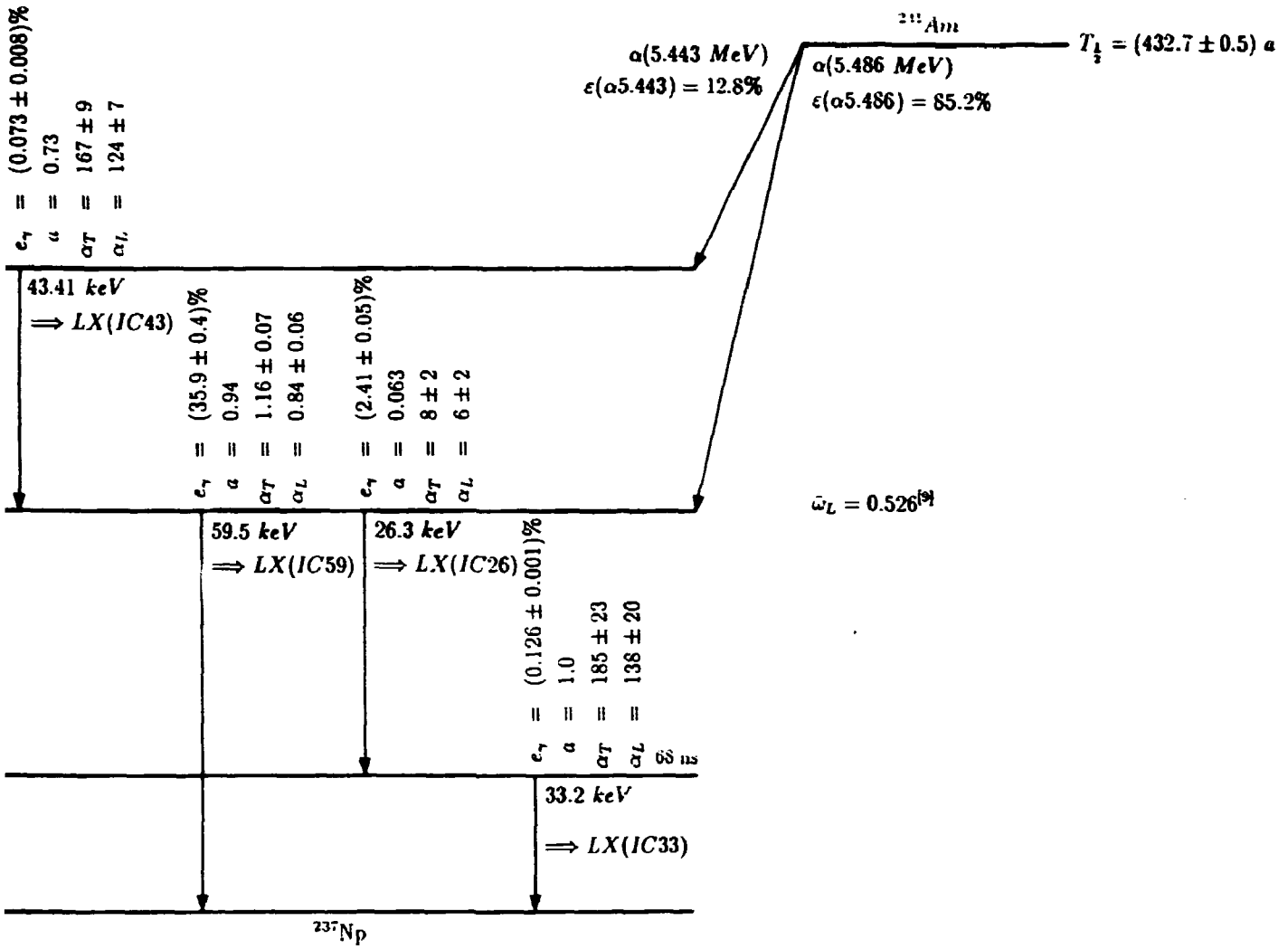

L X-rays	E_x (keV)	e_x (%)
L_ℓ	11.871	0.81±0.10
L_α	13.927	13.0±1.2
$L_\eta + L_\beta$	17.58	20.5±2.4
L_γ	20.997	5.2±0.7

Refer to the text for COI-calculation.

Fig. 16. Decay scheme of ^{241}Am.

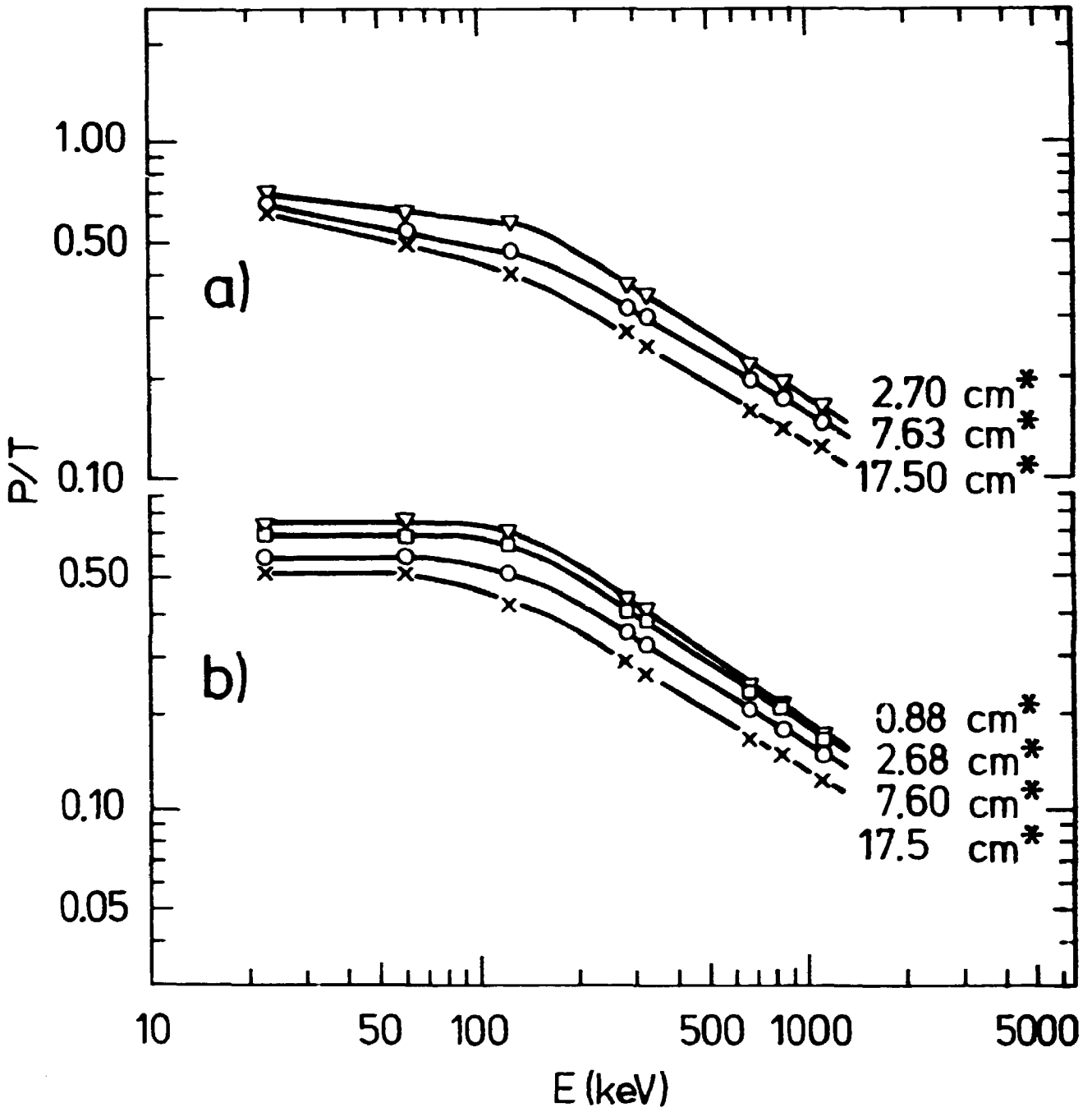

Fig. 17. P/T-curves
a) P/T-curves at 3 positions with a 10-mm perspex absorber
b) P/T-curves at 4 positions without perspex absorber
* distances from the detector face (refer to Table 3)

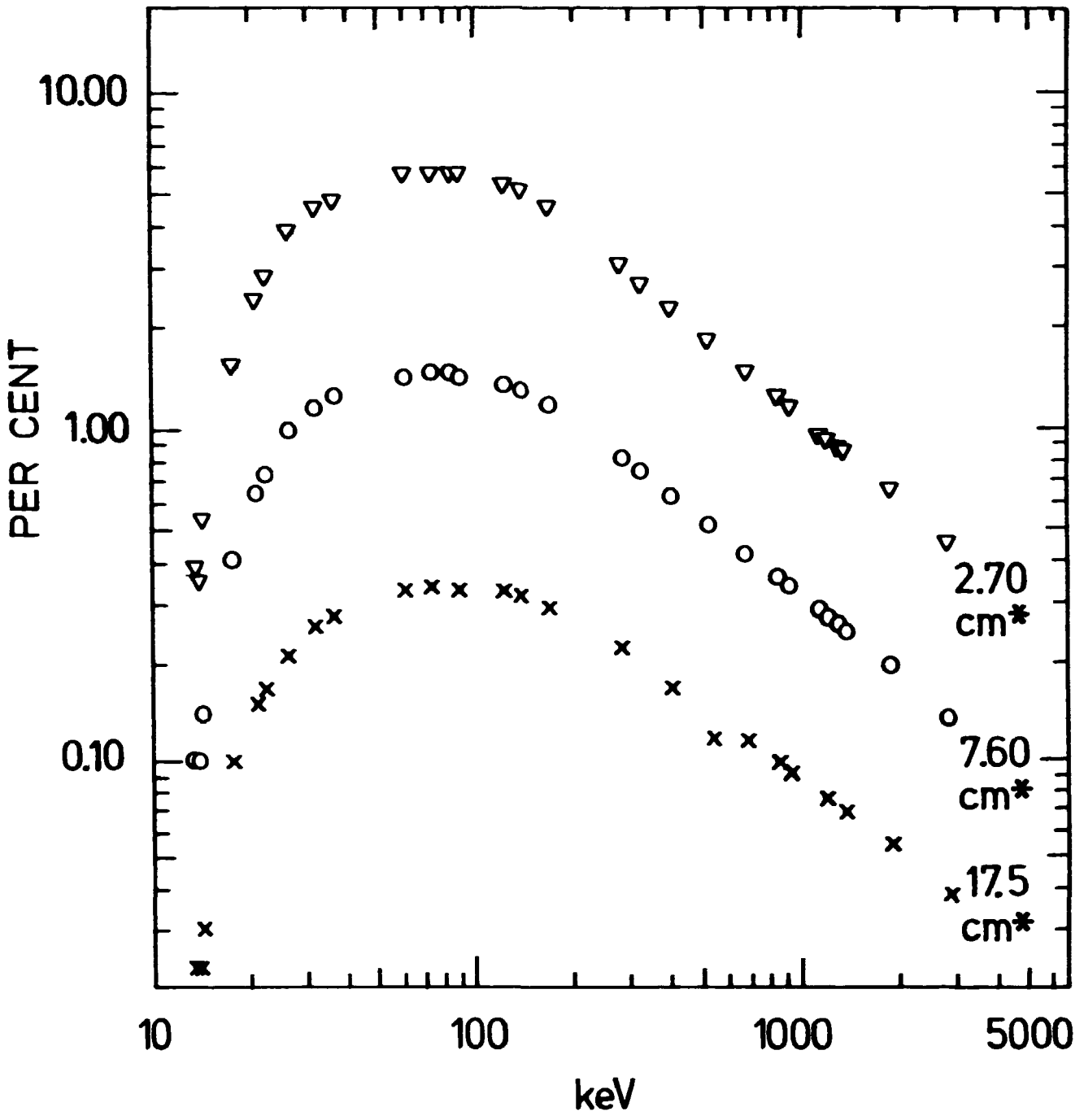

Fig. 18. ε_p-curves determined at 3 positions with a 10-mm perspex absorber
* distances from the detector face (refer to Table 3)

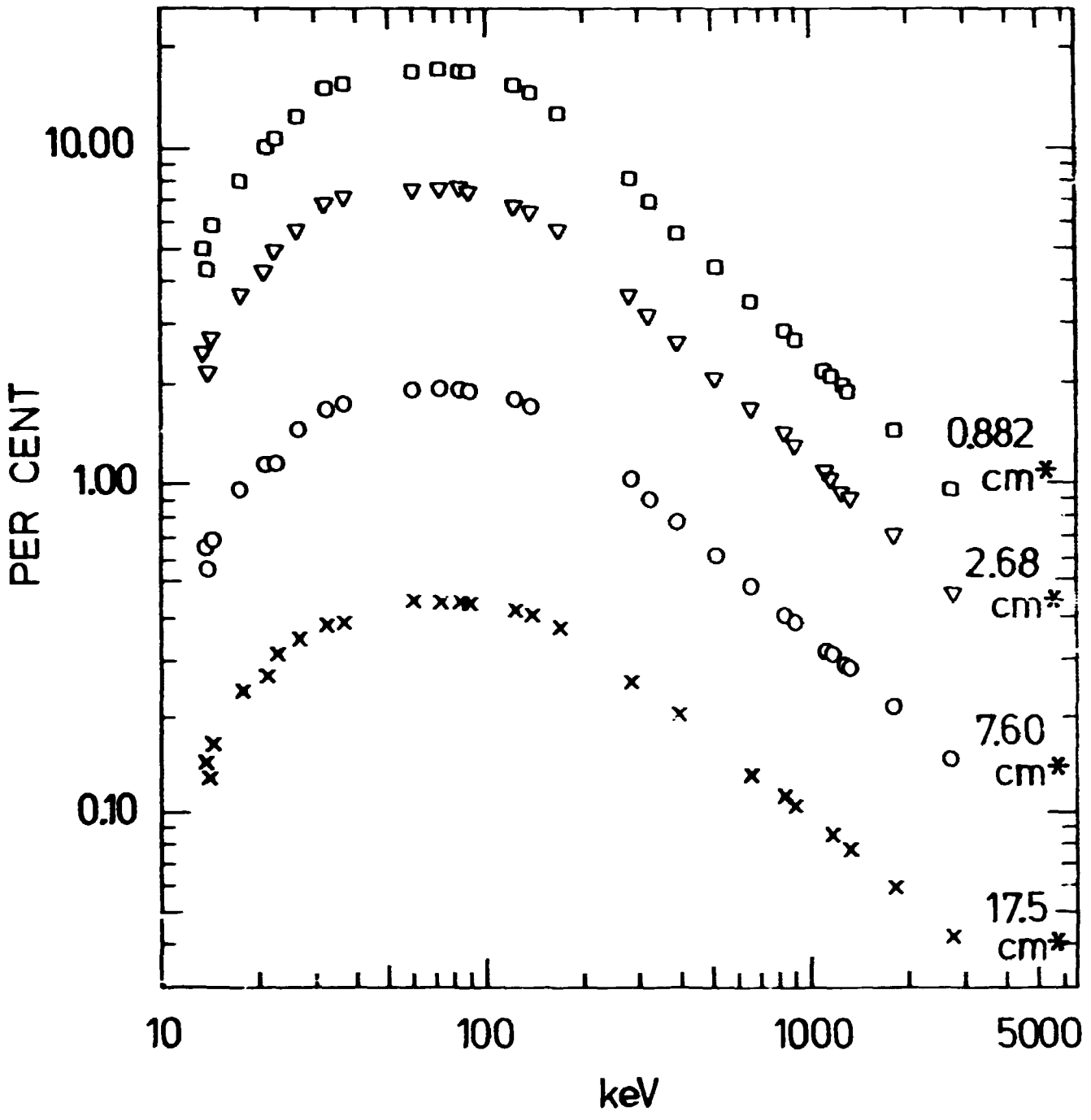

Fig. 19. ε_p-curves determined at 4 positions without perspex absorber
* distances from the detector face (refer to Table 3)

Risø National Laboratory

Risø – R – 593

Title and author(s)

Correction for X- and γ-ray coincidence effects in the efficiency calibration of an n-type germanium detector

Lin Xilei and K. Heydorn

Date June 1991

Department or group

Isotope Division

Groups own registration number(s)

Project/contract no.

Pages 57 Tables 3 Illustrations 19 References 13

ISBN 87-550-1753-3

Abstract (Max. 2000 char.)

The absolute full-energy peak efficiency (ε_p) is an essential parameter in work related to the determination of gamma-ray intensities. ε_p may be determined by means of radioactive standard point sources with single or multiple gamma energies covering the range of interest. Cascade coincidence effects may be avoided by counting point sources 15 cm or more from the detector; however, the efficiency of actual samples measured at positions closer to the detector may have to be determined by means of standard sources of the same geometry and with similar main components as the actual sample.

For n-type gamma-X detectors the situation is particularly difficult. Even single gamma-ray standard sources useful for calibration of p-type gamma-ray detectors cannot always be assumed to be coincidence-free; this is due to the much higher efficiency for X-rays, resulting in gamma-X coincidence effects when counting close to an n-type detector.

This work includes the study of combinations of cascade coincidences between gamma-rays, X-rays, and 511 keV annihilation radiation, as well as β-radiation and its associated bremsstrahlung. The radionuclides ^{22}Na, ^{24}Na, ^{51}Cr, ^{54}Mn, ^{57}Co, ^{60}Co, ^{65}Zn, ^{85}Sr, ^{88}Y, ^{109}Cd, ^{113}Sn, ^{137}Cs, ^{139}Ce, ^{203}Hg, and ^{241}Am were scrutinized for potential cascade coincidences, and practical corrections were calculated.

A gamma-X detector with a relative efficiency of 35 % was calibrated with these 15 nuclides in 1 cm^3 aqueous solutions in half-dram polyethylene containers at 7 distances, ranging from 0.88 cm to 17.5 cm, with and without a perspex β-absorber between the detector and sample. After correcting for coincidences, smooth ε_p-curves were obtained for the energy range 12 to 2750 keV, even for the position closest to the detector.

Descriptors

CALIBRATION; COINCIDENCE SPECTROMETRY; GAMMA DETECTION; GAMMA CASCADES; GE SEMICONDUCTOR DETECTORS; X-RAY DETECTION

Available on request from Risø Library, Risø National Laboratory, (Risø Bibliotek, Forskningscenter Risø), P.O. Box 49, DK-4000 Roskilde, Denmark.
Telephone 02 37 12 12, ext. 2262. Telex: 43116, Telefax: 02 36 06 09

Sales distributors:
G.E.C. Gad Strøget
Vimmelskaftet 32
DK-1161 Copenhagen K, Denmark

Available on exchange from:
Risø Library,
Risø National Laboratory,
P.O. Box 49, DK-4000 Roskilde, Denmark
Phone 42 37 12 12, ext. 2268/2269
Telex 43 116, Telefax 46 75 56 27

ISBN 87-550-1753-3
ISSN 0106-2840